Chapter 1. Interagency Monitoring of Protected Visual Environments (IMPROVE) Network: Configuration and Measurements

1.1 INTRODUCTION

The Regional Haze Rule (RHR), promulgated by the U.S. Environmental Protection Agency (EPA) in 1999 (EPA, 1999a), requires monitoring in locations representative of the 156 visibility-protected federal Class I areas (CIAs, see Figure 1.1) in order to track progress toward the goal of returning visibility to natural conditions. Air quality monitoring under the RHR began in 2000. The most recent RHR guidelines stipulate tracking progress using the haze metric in deciview units on the most anthropogenically impaired days (EPA, 2018), calculated from speciated particle composition concentrations. Computing haze metrics from particle speciation data requires sampling and analysis of major aerosol species, using methods employed by the Interagency Monitoring of Protected Visual Environments (IMPROVE) network since 1987 (Joseph et al., 1987; Malm et al., 1994). These methods are consistent with the aerosol monitoring portion of the 1999 Visibility Monitoring Guidance document issued by the EPA (EPA, 1999b).

The IMPROVE program is a cooperative measurement effort designed to

1. establish current visibility and aerosol conditions in mandatory CIAs;
2. identify chemical species and emission sources responsible for existing anthropogenic and natural visibility impairment;
3. document long-term trends for assessing progress toward the national visibility goal;
4. provide regional haze monitoring representing all visibility-protected federal CIAs where practical.

Although the program is focused on visibility objectives, the data acquired and the methodologies developed by the IMPROVE network have been broadly used to address air quality management related to human health, climate change, ecosystem degradation, and material damage.

The program is managed by the IMPROVE steering committee, which consists of representatives from the EPA; the four federal land managers (FLMs): the National Park Service (NPS), U.S. Forest Service (USFS), U.S. Fish and Wildlife Service (FWS), and Bureau of Land Management (BLM); the National Oceanic and Atmospheric Administration (NOAA); four organizations representing state air quality organizations: the National Association of Clean Air Agencies (NACAA), Western States Air Resource Council/Western Regional Air Partnership (WESTAR/WRAP), Northeast States for Coordinated Air Use Management (NESCAUM), and Mid-Atlantic Regional Air Management Association (MARAMA); and three associate members: the State of Arizona Department of Environmental Quality, Environment Canada, and the South Korea Ministry of Environment.

Also included in this report is a summary of monitoring and data from the EPA's Chemical Speciation Network (CSN). This network exists to monitor aerosol speciation data for understanding human exposure in urban and suburban regions. Aggregating data from the CSN

and the IMPROVE network provides a more complete understanding of current and changing conditions in aerosol composition and haze across the United States.

Figure 1.1. Class I areas of the United States. Shading identifies the managing agency of each CIA.

1.2 OVERVIEW OF THE IMPROVE MONITORING NETWORK

1.2.1 Site Locations

The IMPROVE network initially consisted of 30 monitoring sites in CIAs; twenty of these sites began operation in 1987, followed by the others in the early 1990s. An additional ~40 sites, most in remote areas, that used the same instrumentation, monitoring, and analysis protocols (called IMPROVE protocol sites) began operation prior to 2000 and were separately sponsored by individual federal or state organizations, though they were operated identically to other sites in the IMPROVE network. Adjustments to the number of monitoring sites in the network or the suite of measurements collected at an individual site occurred on several occasions, due in some cases to scientific considerations and in others to resource and funding limitations. Several of the sites also included optical monitoring with a nephelometer or a transmissometer and scene monitoring with color photography to document scenic appearance. The current state of optical monitoring is detailed in Section 1.2.3.

In 1998 the EPA increased its support of IMPROVE to expand the network in CIAs to provide the monitoring required under the RHR. Details regarding the selection process of additional sites was provided in IMPROVE report III (Malm et al., 2000). The selection process was completed by the end of 1999 and installations began shortly thereafter. The network consists of 229 sites (159 operating and 70 discontinued), including representative sites for the CIAs, and additional protocol sites to fill in the spatial gaps where CIAs are sparse or absent. The sites are grouped by region, a semiquantitative empirical categorization that regionally organizes sites based on similar aerosol species concentrations and seasonal patterns. There are 36 IMPROVE regions: 29 rural, four urban (including both long-term urban sites and urban quality assurance sites), and three international sites. Some rural regions may have only one site (e.g., Death Valley, Lone Peak, Virgin Islands). A map of the site locations is provided in Figure 1.2, and a list of sampling sites is provided in Table 1.1, which includes the site name, site code, state, latitude, longitude, elevation, and dates of operation. The sites are depicted by their site code and shaded based on their region, as defined in Table 1.1. Blue symbols correspond to sites with data used in the analyses presented in this report. CIAs and their representative sites are listed in Table 1.2.

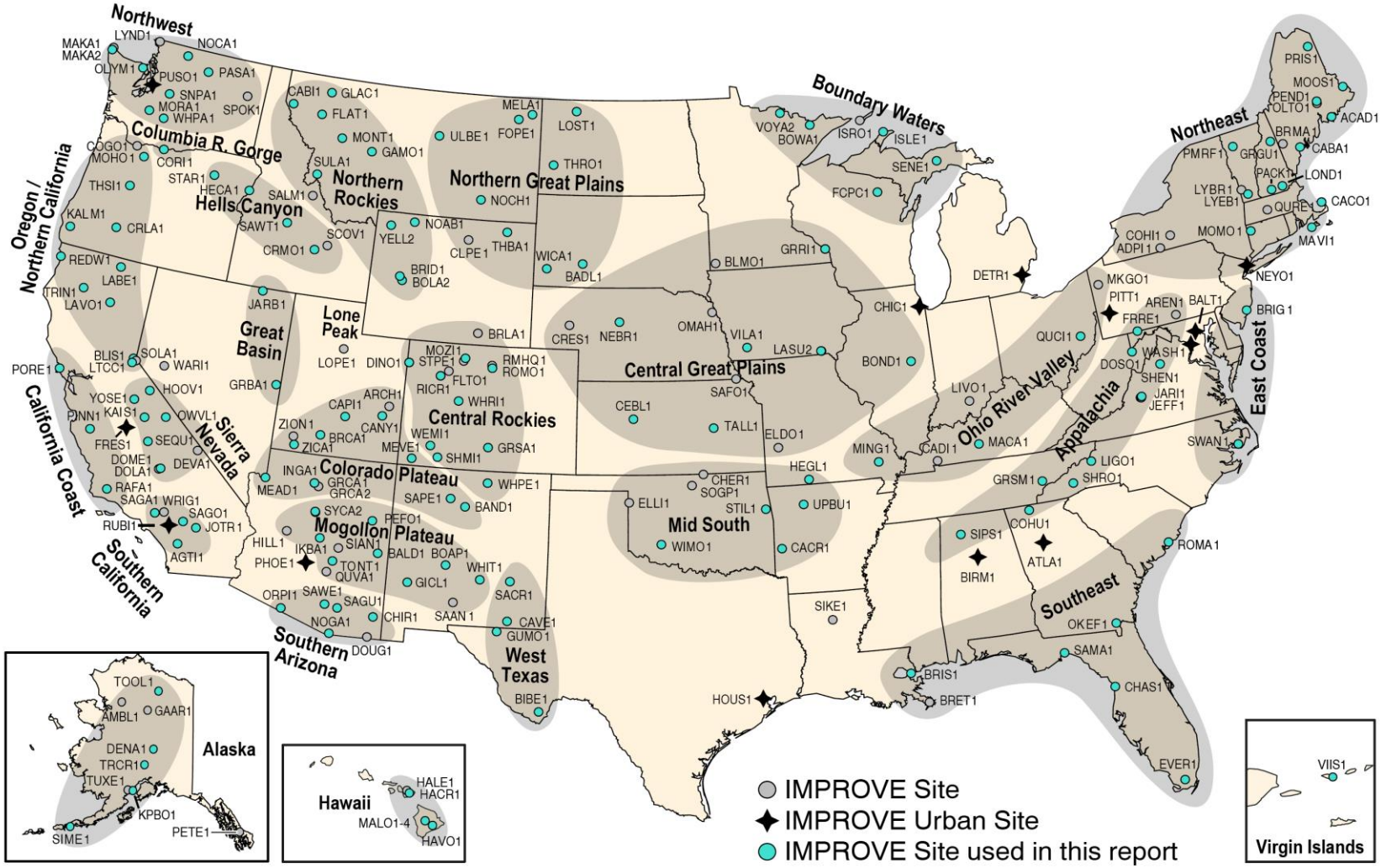

Figure 1.2. Locations of IMPROVE sites for all discontinued and current sites. IMPROVE regions are indicated by shading and bold text. Urban IMPROVE sites are identified by stars. Blue circles indicate sites with data used in the analyses in this report.

Table 1.1. Currently operating and discontinued IMPROVE particulate monitoring sites. Sites are grouped by region, as displayed in Figure 1.2.

Site Name	Site Code	State	Latitude	Longitude	Elevation (m)	Dates of Operation
Alaska						
Ambler	AMBL1	AK	67.099	-157.863	77	09/03/2003-11/29/2004
Denali NP	DENA1	AK	63.723	-148.968	658	03/02/1988-present
Gates of the Arctic NP	GAAR1	AK	66.903	-151.517	196	11/02/2008-10/30/2015
Kenai Peninsula Borough	KPBO1	AK	60.012	-151.711	5	08/19/2015-present
Petersburg	PETE1	AK	56.611	-132.812	0	07/02/2004-09/28/2009
Simeonof	SIME1	AK	55.325	-160.506	57	09/13/2001-present
Toolik Lake Field Station	TOOL1	AK	68.632	-149.606	740	11/01/2018-present
Trapper Creek	TRCR1	AK	62.315	-150.316	155	09/13/2001-present
Tuxedni	TUXE1	AK	59.992	-152.666	15	12/03/2001-01/12/2015
Alberta						
Barrier Lake	BALA1	AB	51.029	-115.034	1391	01/15/2011-03/29/2017
Appalachia						
Arendtsville	AREN1	PA	39.923	-77.308	267	04/04/2001-12/31/2010
Cohutta	COHU1	GA	34.785	-84.626	735	06/03/2000-present
Dolly Sods WA	DOSO1	WV	39.105	-79.426	1182	09/04/1991-present
Frostburg Reservoir	FRRE1	MD	39.706	-79.012	767	03/01/2004-present
Great Smoky Mountains NP	GRSM1	TN	35.633	-83.942	810	03/02/1988-present
James River Face WA	JARI1	VA	37.627	-79.513	290	06/03/2000-present
Jefferson NF	JEFF1	VA	37.617	-79.483	219	09/1994-02/26/2000
Linville Gorge WA	LIGO1	NC	35.972	-81.933	969	04/01/2000-present
Shenandoah NP	SHEN1	VA	38.523	-78.435	1079	03/02/1988-present
Shining Rock WA	SHRO1	NC	35.394	-82.774	1617	06/01/1994-present
Sipsey WA	SIPS1	AL	34.343	-87.339	286	03/04/1992-present
Boundary Waters						
Boundary Waters Canoe Area WA	BOWA1	MN	47.947	-91.496	527	06/01/1991-present
Forest County Potawatomi Community	FCPC1	WI	45.565	-88.808	564	11/17/2016-present
Isle Royale NP	ISLE1	MI	47.46	-88.149	182	11/17/1999-present
Isle Royale NP	ISRO1	MI	47.917	-89.15	213	06/01/1988-12/29/1999
Seney	SENE1	MI	46.289	-85.95	215	11/17/1999-present
Voyageurs NP #1	VOYA1	MN	48.413	-92.83	426	03/02/1988-12/29/1999
Voyageurs NP #2	VOYA2	MN	48.413	-92.829	429	03/02/1999-present
California Coast						
Pinnacles NP	PINN1	CA	36.483	-121.157	302	03/02/1988-present
Point Reyes NS	PORE1	CA	38.122	-122.909	97	03/02/1988-present
San Rafael WA	RAFA1	CA	34.734	-120.007	956	02/02/2000-present
Central Great Plains						
Blue Mounds	BLMO1	MN	43.716	-96.191	473	06/01/2002-12/29/2015
Bondville	BOND1	IL	40.052	-88.373	263	03/08/2001-present
Cedar Bluff	CEBL1	KS	38.77	-99.763	666	06/01/2002-present
Crescent Lake	CRES1	NE	41.763	-102.434	1207	06/01/2002-12/29/2015
El Dorado Springs	ELDO1	MO	37.701	-94.035	298	03/03/2002-12/29/2015
Great River Bluffs	GRRI1	MN	43.937	-91.405	370	06/01/2002-present

Site Name	Site Code	State	Latitude	Longitude	Elevation (m)	Dates of Operation
Lake Sugema #1	LASU1	IA	40.688	-91.988	210	05/08/2002-11/29/2004
Lake Sugema #2	LASU2	IA	40.693	-92.006	229	12/02/2004-present
Nebraska NF	NEBR1	NE	41.889	-100.339	883	06/01/2002-present
Omaha	OMAH1	NE	42.149	-96.432	430	06/02/2003-08/04/2008
Sac and Fox	SAFO1	KS	39.979	-95.568	293	06/01/2002-06/29/2011
Tallgrass	TALL1	KS	38.434	-96.56	390	09/02/2002-present
Viking Lake	VILA1	IA	40.969	-95.045	371	05/08/2002-present
Central Rocky Mountains						
Brooklyn Lake	BRLA1	WY	41.366	-106.242	3196	07/31/1993-01/31/2004
Dinosaur NM	DINO1	CO	40.25	-108.967	1829	11/01/2018-present
Fort Collins	FOCO1	CO	40.593	-105.143	1572	07/2020-present
Fort Collins	FOCO2	CO	40.593	-105.143	1572	07/2020-present
Flat Tops	FLTO1	CO	39.915	-107.635	2593	10/27/2011-09/28/2021
Great Sand Dunes NP	GRSA1	CO	37.725	-105.519	2498	03/02/1988-present
Mount Zirkel WA	MOZI1	CO	40.538	-106.677	3243	06/01/1994-present
Ripple Creek	RICR1	CO	40.087	-107.314	2934	03/02/2009-10/30/2011
Rocky Mountain NP Headquarters	RMHQ1	CO	40.362	-105.564	2408	03/02/1988-12/29/1999
Rocky Mountain NP	ROMO1	CO	40.278	-105.546	2760	09/01/1990-present
Storm Peak	STPE1	CO	40.445	-106.74	3220	12/01/1993-12/29/1999
Shamrock Mine	SHMI1	CO	37.304	-107.484	2351	08/01/2004-12/27/2021
Wheeler Peak	WHPE1	NM	36.585	-105.452	3366	08/16/2000-present
White River NF	WHRI1	CO	39.154	-106.821	3414	06/02/1993-present
Colorado Plateau						
Arches NP	ARCH1	UT	38.783	-109.583	1722	03/02/1988-12/29/1999
Bandelier NM	BAND1	NM	35.78	-106.266	1988	03/02/1988-present
Bryce Canyon NP	BRCA1	UT	37.618	-112.174	2481	03/02/1988-present
Canyonlands NP	CANY1	UT	38.459	-109.821	1798	03/02/1988-present
Capitol Reef NP	CAPI1	UT	38.302	-111.293	1896	04/19/2000-present
Hopi Point	GRCA1	AZ	36.066	-112.154	2164	03/02/1988-12/29/1999
Hance Camp at Grand Canyon NP	GRCA2	AZ	35.973	-111.984	2267	03/02/1996-present
Indian Gardens	INGA1	AZ	36.078	-112.129	1166	09/02/1989-05/13/2013
Meadview	MEAD1	AZ	36.019	-114.068	902	09/04/1991-02/27/2021
Mesa Verde NP	MEVE1	CO	37.198	-108.491	2172	03/02/1988-present
San Pedro Parks WA	SAPE1	NM	36.014	-106.845	2935	08/16/2000-present
Weminuche WA	WEMI1	CO	37.659	-107.8	2750	03/02/1988-present
Zion Canyon	ZICA1	UT	37.198	-113.151	1215	12/01/2002-present
Zion NP	ZION1	UT	37.459	-113.224	1545	03/25/2000-08/22/2004
Columbia River Gorge						
Columbia Gorge	COGO1	WA	45.569	-122.21	230	09/18/1996-10/30/2011
Columbia River Gorge	CORI1	WA	45.664	-121.001	178	06/02/1993-present
Death Valley						
Death Valley NP	DEVA1	CA	36.509	-116.848	130	09/04/1993-04/28/2013
East Coast						
Brigantine NWR	BRIG1	NJ	39.465	-74.449	5	09/04/1991-present
Swanquarter	SWAN1	NC	35.451	-76.208	-4	06/10/2000-present
Great Basin						
Great Basin NP	GRBA1	NV	39.005	-114.216	2066	03/04/1992-present
Jarbidge WA	JARB1	NV	41.893	-115.426	1869	03/02/1988-present
Hawaii						

Site Name	Site Code	State	Latitude	Longitude	Elevation (m)	Dates of Operation
Haleakala Crater	HACR1	HI	20.759	-156.248	2158	01/24/2007-present
Haleakala NP	HALE1	HI	20.809	-156.282	1153	12/01/1990-05/30/2012
Hawaii Volcanoes NP	HAVO1	HI	19.431	-155.258	1259	03/02/1988-present
Mauna Loa Observatory #1	MALO1	HI	19.536	-155.577	3439	12/02/1992-08/28/2004
Mauna Loa Observatory #2	MALO2	HI	19.536	-155.577	3439	12/02/1992-08/28/2004
Mauna Loa Observatory #3	MALO3	HI	19.539	-155.578	3400	03/06/1996-02/26/2000
Mauna Loa Observatory #4	MALO4	HI	19.539	-155.578	3400	03/02/1996-02/26/2000
Hells Canyon						
Craters of the Moon NM	CRMO1	ID	43.461	-113.555	1818	03/04/1992-present
Hells Canyon	HECA1	OR	44.97	-116.844	655	09/03/2000-present
Sawtooth NF	SAWT1	ID	44.171	-114.927	1990	12/01/1993-present
Scoville	SCOV1	ID	43.65	-113.033	1500	03/04/1992-02/26/2000
Starkey	STAR1	OR	45.225	-118.513	1259	03/15/2000-present
Korea						
Baengnyeong Island	BYIS1		37.966	124.631	100	03/20/2013-present
Lone Peak						
Lone Peak WA	LOPE1	UT	40.445	-111.708	1768	12/01/1993-08/29/2001
Mid South						
Caney Creek	CACR1	AR	34.454	-94.143	683	06/24/2000-present
Cherokee Nation	CHER1	OK	36.956	-97.031	342	09/02/2002-04/20/2010
Ellis	ELLI1	OK	36.085	-99.935	697	03/02/2002-10/18/2015
Hercules-Glades	HEGL1	MO	36.614	-92.922	404	03/02/2001-present
Sikes	SIKE1	LA	32.057	-92.435	45	03/02/2001-12/31/2010
Southern Great Plains	SOGP1	OK	36.605	-97.485	315	10/01/2019-present
Stilwell	STIL1	OK	35.75	-94.67	300	04/23/2010-present
Upper Buffalo WA	UPBU1	AR	35.826	-93.203	723	12/24/1991-present
Wichita Mountains	WIMO1	OK	34.732	-98.713	509	03/02/2001-present
Mogollon Plateau						
Mount Baldy	BALD1	AZ	34.058	-109.441	2509	03/01/2000-present
Bosque del Apache	BOAP1	NM	33.87	-106.852	1390	04/15/2000-present
Gila WA	GICL1	NM	33.22	-108.235	1776	03/02/1994-present
Hillside	HILL1	AZ	34.429	-112.963	1511	04/19/2001-05/31/2005
Ike's Backbone	IKBA1	AZ	34.341	-111.683	1298	03/29/2000-present
Petrified Forest NP	PEFO1	AZ	35.078	-109.769	1766	03/02/1988-present
San Andres	SAAN1	NM	32.687	-106.484	1326	07/30/1997-02/26/2000
Sierra Ancha	SIAN1	AZ	34.091	-110.942	1600	02/09/2000-12/03/2017
Sycamore Canyon #1	SYCA1	AZ	35.141	-111.969	2046	09/04/1991-10/30/2015
Sycamore Canyon #2	SYCA2	AZ	35.164	-111.982	2046	10/24/2015-present
Tonto	TONT1	AZ	33.655	-111.107	775	03/02/1988-present
White Mountain	WHIT1	NM	33.469	-105.535	2064	12/03/2001-present
Northeast						
Acadia NP	ACAD1	ME	44.377	-68.261	157	03/02/1988-present
Addison Pinnacle	ADPI1	NY	42.091	-77.21	512	04/04/2001-06/28/2010
Bridgton	BRMA1	ME	44.107	-70.729	234	03/14/2001-12/29/2015
Casco Bay	CABA1	ME	43.833	-70.064	27	03/14/2001-present
Cape Cod	CACO1	MA	41.976	-70.024	49	04/04/2001-present

Site Name	Site Code	State	Latitude	Longitude	Elevation (m)	Dates of Operation
Connecticut Hill	COHI1	NY	42.401	-76.653	519	04/04/2001-06/25/2006
Great Gulf WA	GRGU1	NH	44.308	-71.218	454	06/03/1995-present
Londonderry	LOND1	NH	42.862	-71.380	124	01/03/2011-present
Lye Brook WA	LYBR1	VT	43.148	-73.127	1015	09/04/1991-09/30/2012
Lye Brook WA	LYEB1	VT	42.956	-72.91	882	01/01/2012-present
Martha's Vineyard	MAVI1	MA	41.331	-70.785	3	12/01/2002-present
Mohawk Mt.	MOMO1	CT	41.821	-73.297	522	09/13/2001-present
Moosehorn NWR	MOOS1	ME	45.126	-67.266	78	12/03/1994-present
Old Town	OLTO1	ME	44.933	-68.646	51	06/27/2001-05/29/2006
Pack Monadnock Summit	PACK1	NH	42.862	-71.879	695	10/03/2007-present
Penobscot	PENO1	ME	44.948	-68.648	45	01/11/2006-present
Proctor Maple Research Facility	PMRF1	VT	44.528	-72.869	401	12/01/1993-present
Presque Isle	PRIS1	ME	46.696	-68.033	166	03/08/2001-present
Quabbin Summit	QURE1	MA	42.298	-72.335	318	04/04/2001-12/29/2015
Northern Great Plains						
Badlands NP	BADL1	SD	43.743	-101.941	736	03/02/1988-present
Cloud Peak	CLPE1	WY	44.334	-106.957	2471	06/01/2002-07/29/2015
Fort Peck	FOPE1	MT	48.308	-105.102	638	06/01/2002-present
Lostwood	LOST1	ND	48.642	-102.402	696	12/15/1999-present
Medicine Lake	MELA1	MT	48.487	-104.476	606	12/15/1999-present
Northern Cheyenne	NOCH1	MT	45.65	-106.557	1283	06/01/2002-present
Thunder Basin	THBA1	WY	44.663	-105.287	1195	06/01/2002-12/29/2019
Theodore Roosevelt NP	THRO1	ND	46.895	-103.378	853	12/15/1999-present
UL Bend	ULBE1	MT	47.582	-108.72	891	01/26/2000-present
Wind Cave NP	WICA1	SD	43.558	-103.484	1296	12/15/1999-present
Northern Rocky Mountains						
Boulder Lake	BOLA1	WY	42.846	-109.640	2296	08/26/2009-present
Bridger WA	BRID1	WY	42.975	-109.758	2627	03/02/1988-present
Cabinet Mountains	CABI1	MT	47.955	-115.671	1441	07/26/2000-present
Flathead	FLAT1	MT	47.773	-114.269	1580	06/01/2002-present
Gates of the Mountains	GAMO1	MT	46.826	-111.711	2387	07/26/2000-present
Glacier NP	GLAC1	MT	48.511	-113.997	975	03/02/1988-present
Monture	MONT1	MT	47.122	-113.154	1282	03/29/2000-present
North Absaroka	NOAB1	WY	44.745	-109.382	2482	01/26/2000-present
Salmon NF	SALM1	ID	45.159	-114.026	2788	12/01/1993-11/05/2000
Sula Peak	SULA1	MT	45.86	-114	1896	06/01/1994-present
Yellowstone NP #1	YELL1	WY	44.565	-110.4	2442	03/09/1988-12/29/1999
Yellowstone NP #2	YELL2	WY	44.565	-110.4	2425	03/02/1988-present
Northwest						
Lynden	LYND1	WA	48.953	-122.559	28	10/16/1996-12/29/1999
Makah Indian Reservation #1	MAKA1	WA	48.372	-124.595	9	09/02/2006-10/29/2010
Makah Indian Reservation #2	MAKA2	WA	48.298	-124.625	480	11/01/2010-present
Mount Rainier NP	MORA1	WA	46.758	-122.124	439	03/02/1988-present
North Cascades	NOCA1	WA	48.732	-121.065	568	07/30/1997-present
Olympic NP	OLYM1	WA	48.007	-122.973	599	07/12/2001-present
Pasayten	PASA1	WA	48.388	-119.928	1627	11/02/2000-present
Snoqualmie Pass	SNPA1	WA	47.422	-121.426	1049	06/02/1993-present

Site Name	Site Code	State	Latitude	Longitude	Elevation (m)	Dates of Operation
Spokane Reservation	SPOK1	WA	47.905	-117.861	552	07/12/2001-06/30/2005
White Pass	WHPA1	WA	46.624	-121.388	1827	02/16/2000-present
Not Assigned						
Walker River Paiute Tribe	WARI1	NV	38.952	-118.815	1250	06/02/2003-10/31/2005
Ohio River Valley						
Cadiz	CADI1	KY	36.784	-87.85	192	03/08/2001-12/31/2010
Livonia	LIVO1	IN	38.535	-86.26	281	03/08/2001-12/31/2010
Mammoth Cave NP	MACA1	KY	37.132	-86.148	235	09/04/1991-present
Mingo	MING1	MO	36.972	-90.143	111	06/03/2000-present
M.K. Goddard	MKGO1	PA	41.427	-80.145	380	04/04/2001-12/31/2010
Quaker City	QUCI1	OH	39.943	-81.338	366	04/04/2001-present
Ontario						
Egbert	EGBE1	ON	44.231	-79.783	251	9/01/2005-present
Oregon and Northern California						
Bliss SP	BLIS1	CA	38.976	-120.103	2131	09/01/1990-present
Crater Lake NP	CRLA1	OR	42.896	-122.136	1996	03/02/1988-present
Kalmiopsis	KALM1	OR	42.552	-124.059	80	03/11/2000-present
Lava Beds NM	LABE1	CA	41.712	-121.507	1460	03/29/2000-present
Lassen Volcanic NP	LAVO1	CA	40.54	-121.577	1733	03/02/1988-present
Lake Tahoe Community College	LTCC1	CA	38.925	-119.98	1935	02/19/2014-present
Mount Hood	MOHO1	OR	45.289	-121.784	1531	03/15/2000-present
Redwood NP	REDW1	CA	41.561	-124.084	244	03/02/1988-present
Three Sisters WA	THSI1	OR	44.291	-122.043	885	06/02/1993-present
Trinity	TRIN1	CA	40.786	-122.805	1014	10/18/2000-present
Phoenix						
Phoenix	PHOE1	AZ	33.504	-112.096	342	04/19/2001-present
Phoenix	PHOE5	AZ	33.504	-112.096	342	01/01/2005-present
Puget Sound						
Puget Sound	PUSO1	WA	47.57	-122.312	98	03/02/1996-present
Sierra Nevada						
Dome Lands WA	DOLA1	CA	35.699	-118.202	914	06/01/1994-12/29/1999
Dome Lands WA	DOME1	CA	35.728	-118.138	927	02/02/2000-present
Hoover	HOOV1	CA	38.088	-119.177	2561	06/06/2001-present
Kaiser	KAIS1	CA	37.221	-119.155	2598	01/26/2000-present
Owens Valley	OWVL1	CA	37.361	-118.331	1234	06/27/2013-present
Sequoia NP	SEQU1	CA	36.489	-118.829	519	03/04/1992-present
South Lake Tahoe	SOLA1	CA	38.933	-119.967	1900	03/01/1989-12/29/1999
Yosemite NP	YOSE1	CA	37.713	-119.706	1603	03/02/1988-present
Southeast						
Breton	BRET1	LA	29.119	-89.207	11	08/16/2000-08/29/2005
Breton Island	BRIS1	LA	30.109	-89.762	-7	01/16/2008-present
Chassahowitzka NWR	CHAS1	FL	28.748	-82.555	4	03/03/1993-present
Everglades NP	EVER1	FL	25.391	-80.681	1	09/03/1988-present
Okefenokee NWR	OKEF1	GA	30.741	-82.128	48	09/04/1991-present
Cape Romain NWR	ROMA1	SC	32.941	-79.657	5	09/03/1994-present
St. Marks NWR	SAMA1	FL	30.093	-84.161	7	08/16/2000-present
Southern Arizona						
Chiricahua NM	CHIR1	AZ	32.009	-109.389	1555	03/02/1988-present
Douglas	DOUG1	AZ	31.349	-109.54	1230	06/02/2004-10/30/2015
Nogales	NOGA1	AZ	31.338	-110.937	1172	10/27/2015-present

Site Name	Site Code	State	Latitude	Longitude	Elevation (m)	Dates of Operation
Organ Pipe	ORPI1	AZ	31.951	-112.802	504	12/01/2002-present
Queen Valley	QUVA1	AZ	33.294	-111.286	661	04/19/2001-12/29/2015
Saguaro NP	SAGU1	AZ	32.175	-110.737	941	06/01/1988-present
Saguaro West	SAWE1	AZ	32.249	-111.218	714	10/31/2001-present
Southern California						
Agua Tibia	AGTI1	CA	33.464	-116.971	508	12/20/2000-present
Joshua Tree NP	JOSH1	CA	34.069	-116.389	1235	02/23/2000-present
Joshua Tree NP	JOTR1	CA	34.069	-116.389	1228	09/04/1991-12/29/1999
San Gabriel	SAGA1	CA	34.297	-118.028	1791	12/03/2001-present
San Gorgonio WA	SAGO1	CA	34.194	-116.913	1726	03/02/1988-present
Wrightwood	WRIG1	CA	34.38	-117.69	2106	10/01/2009-10/15/2012
Urban Quality Assurance Sites						
Atlanta	ATLA1	GA	33.688	-84.29	243	03/01/2004-present
Baltimore	BALT1	MD	39.255	-76.709	78	06/02/2004-12/31/2006
Birmingham	BIRM1	AL	33.553	-86.815	176	03/01/2004-present
Chicago	CHIC1	IL	41.751	-87.713	195	09/03/2003-08/29/2005
Detroit	DETR1	MI	42.229	-83.209	180	09/03/2003-present
Fresno	FRES1	CA	36.782	-119.773	100	09/03/2004-present
Houston	HOUS1	TX	29.67	-95.129	7	03/01/2004-08/29/2005
New York City	NEYO1	NY	40.816	-73.902	45	08/01/2004-06/07/2010
Pittsburgh	PITT1	PA	40.465	-79.961	268	03/01/2004-present
Rubidoux	RUBI1	CA	34.0	-117.416	248	09/03/2004-08/29/2005
Virgin Islands						
Virgin Islands NP	VIIS1	VI	18.336	-64.796	51	09/01/1990-present
Washington D.C.						
Washington D.C.	WASH1	DC	38.876	-77.034	15	03/02/1988-06/08/2015
West Texas						
Big Bend NP	BIBE1	TX	29.303	-103.178	1067	03/02/1988-present
Carlsbad Caverns NP	CAVE1	NM	32.178	-104.444	1355	07/30/2017-present
Guadalupe Mountains NP	GUMO1	TX	31.833	-104.809	1672	03/02/1988-present
Salt Creek	SACR1	NM	33.46	-104.404	1072	04/08/2000-present

NF = National Forest
NM = National Monument
NP = National Park
NS = National Seashore
NWR = National Wildlife Refuge
SP = State Park
WA = Wilderness Area

Table 1.2. Class I areas and representative monitoring sites.

Class I Area Name	Site Name	Site Code
Acadia	Acadia NP	ACAD1
Agua Tibia	Agua Tibia	AGTI1
Alpine Lakes	Snoqualmie Pass	SNPA1
Anaconda-Pintler	Sula Peak	SULA1
Ansel Adams	Kaiser	KAIS1
Arches	Canyonlands NP	CANY1
Badlands	Badlands NP	BADL1
Bandelier	Bandelier NM	BAND1
Big Bend	Big Bend NP	BIBE1
Black Canyon of the Gunnison	Weminuche WA	WEMI1
Bob Marshall	Monture	MONT1

Class I Area Name	Site Name	Site Code
Bosque del Apache	Bosque del Apache	BOAP1
Boundary Waters Canoe Area	Boundary Waters Canoe Area WA	BOWA1
Breton	Breton	BRIS1
Bridger	Bridger WA	BRID1
Brigantine	Brigantine NWR	BRIG1
Bryce Canyon	Bryce Canyon NP	BRCA1
Cabinet Mountains	Cabinet Mountains	CABI1
Caney Creek	Caney Creek	CACR1
Canyonlands	Canyonlands NP	CANY1
Cape Romain	Cape Romain NWR	ROMA1
Capitol Reef	Capitol Reef NP	CAPI1
Caribou	Lassen Volcanic NP	LAVO1
Carlsbad Caverns	Guadalupe Mountains NP	GUMO1
Chassahowitzka	Chassahowitzka NWR	CHAS1
Chiricahua NM	Chiricahua NM	CHIR1
Chiricahua W	Chiricahua NM	CHIR1
Cohutta	Cohutta	COHU1
Crater Lake	Crater Lake NP	CRLA1
Craters of the Moon	Craters of the Moon NM	CRMO1
Cucamonga	San Gabriel	SAGA1
Denali	Denali NP	DENA1
Desolation	Bliss SP	BLIS1
Diamond Peak	Crater Lake NP	CRLA1
Dolly Sods	Dolly Sods WA	DOSO1
Dome Land	Dome Lands WA	DOME1
Eagle Cap	Starkey	STAR1
Eagles Nest	White River NF	WHRI1
Emigrant	Yosemite NP	YOSE1
Everglades	Everglades NP	EVER1
Fitzpatrick	Bridger WA	BRID1
Flat Tops	White River NF	WHRI1
Galiuro	Chiricahua NM	CHIR1
Gates of the Mountains	Gates of the Mountains	GAMO1
Gearhart Mountain	Crater Lake NP	CRLA1
Gila	Gila WA	GICL1
Glacier	Glacier NP	GLAC1
Glacier Peak	North Cascades	NOCA1
Goat Rocks	White Pass	WHPA1
Grand Canyon	Hance Camp at Grand Canyon NP	GRCA2
Grand Teton	Yellowstone NP	YELL2
Great Gulf	Great Gulf WA	GRGU1
Great Sand Dunes	Great Sand Dunes NP	GRSA1
Great Smoky Mountains	Great Smoky Mountains NP	GRSM1
Guadalupe Mountains	Guadalupe Mountains NP	GUMO1
Haleakala	Haleakala Crater	HACR1
Hawaii Volcanoes	Hawaii Volcanoes NP	HAVO1
Hells Canyon	Hells Canyon	HECA1
Hercules-Glade	Hercules-Glades	HEGL1
Hoover	Hoover	HOOV1
Isle Royale	Isle Royale NP	ISLE1
James River Face	James River Face WA	JARI1
Jarbidge	Jarbidge WA	JARB1
John Muir	Kaiser	KAIS1
Joshua Tree	Joshua Tree NP	JOSH1

Class I Area Name	Site Name	Site Code
Joyce Kilmer-Slickrock	Great Smoky Mountains NP	GRSM1
Kaiser	Kaiser	KAIS1
Kalmiopsis	Kalmiopsis	KALM1
Kings Canyon	Sequoia NP	SEQU1
La Garita	Weminuche WA	WEMI1
Lassen Volcanic	Lassen Volcanic NP	LAVO1
Lava Beds	Lava Beds NM	LABE1
Linville Gorge	Linville Gorge	LIGO1
Lostwood	Lostwood	LOST1
Lye Brook	Lye Brook WA	LYBR1
Mammoth Cave	Mammoth Cave NP	MACA1
Marble Mountain	Trinity	TRIN1
Maroon Bells-Snowmass	White River NF	WHRI1
Mazatzal	Ike's Backbone	IKBA1
Medicine Lake	Medicine Lake	MELA1
Mesa Verde	Mesa Verde NP	MEVE1
Mingo	Mingo	MING1
Mission Mountains	Monture	MONT1
Mokelumne	Bliss SP	BLIS1
Moosehorn	Moosehorn NWR	MOOS1
Mount Adams	White Pass	WHPA1
Mount Baldy	Mount Baldy	BALD1
Mount Hood	Mount Hood	MOHO1
Mount Jefferson	Three Sisters WA	THSI1
Mount Rainier	Mount Rainier NP	MORA1
Mount Washington	Three Sisters WA	THSI1
Mount Zirkel	Mount Zirkel WA	MOZI1
Mountain Lakes	Crater Lake NP	CRLA1
North Absaroka	North Absaroka	NOAB1
North Cascades	North Cascades	NOCA1
Okefenokee	Okefenokee NWR	OKEF1
Olympic	Olympic	OLYM1
Otter Creek	Dolly Sods WA	DOSO1
Pasayten	Pasayten	PASA1
Pecos	Wheeler Peak	WHPE1
Petrified Forest	Petrified Forest NP	PEFO1
Pine Mountain	Ike's Backbone	IKBA1
Pinnacles	Pinnacles NP	PINN1
Point Reyes	Point Reyes NS	PORE1
Presidential Range-Dry River	Great Gulf WA	GRGU1
Rawah	Mount Zirkel WA	MOZI1
Red Rock Lakes	Yellowstone NP	YELL2
Redwood	Redwood NP	REDW1
Rocky Mountain	Rocky Mountain NP	ROMO1
Roosevelt Campobello	Moosehorn NWR	MOOS1
Saguaro	Saguaro NP	SAGU1
Saint Marks	St. Marks	SAMA1
Salt Creek	Salt Creek	SACR1
San Gabriel	San Gabriel	SAGA1
San Gorgonio	San Gorgonio WA	SAGO1
San Jacinto	San Gorgonio WA	SAGO1
San Pedro Parks	San Pedro Parks	SAPE1
San Rafael	San Rafael	RAFA1
Sawtooth	Sawtooth NF	SAWT1

Class I Area Name	Site Name	Site Code
Scapegoat	Monture	MONT1
Selway-Bitterroot	Sula Peak	SULA1
Seney	Seney	SENE1
Sequoia	Sequoia NP	SEQU1
Shenandoah	Shenandoah NP	SHEN1
Shining Rock	Shining Rock WA	SHRO1
Sierra Ancha	Sierra Ancha	SIAN1
Simeonof	Simeonof	SIME1
Sipsey	Sipsey WA	SIPS1
South Warner	Lava Beds NM	LABE1
Strawberry Mountain	Starkey	STAR1
Superstition	Tonto	TONT1
Swanquarter	Swanquarter	SWAN1
Sycamore Canyon	Sycamore Canyon	SYCA1
Teton	Yellowstone NP	YELL2
Theodore Roosevelt	Theodore Roosevelt NP	THRO1
Thousand Lakes	Lassen Volcanic NP	LAVO1
Three Sisters	Three Sisters WA	THSI1
Tuxedni	Kenai Peninsula Borough	KPBO1
UL Bend	UL Bend	ULBE1
Upper Buffalo	Upper Buffalo WA	UPBU1
Ventana	Pinnacles NP	PINN1
Virgin Islands	Virgin Islands NP	VIIS1
Voyageurs	Voyageurs NP	VOYA2
Washakie	North Absaroka	NOAB1
Weminuche	Weminuche WA	WEMI1
West Elk	White River NF	WHRI1
Wheeler Peak	Wheeler Peak	WHPE1
White Mountain	White Mountain	WHIT1
Wichita Mountains	Wichita Mountains	WIMO1
Wind Cave	Wind Cave	WICA1
Wolf Island	Okefenokee NWR	OKEF1
Yellowstone	Yellowstone NP	YELL2
Yolla Bolly-Middle Eel	Trinity	TRIN1
Yosemite	Yosemite NP	YOSE1
Zion	Zion Canyon	ZICA1

NF = National Forest
NM = National Monument
NP = National Park
NS = National Seashore
NWR = National Wildlife Refuge
SP = State Park
WA = Wilderness Area

1.2.2 Aerosol Sampling and Analysis

The current configuration of the IMPROVE monitor collects 24-hour samples every third day from midnight to midnight local standard time and data are reported at local conditions. The samplers have undergone modifications over time (Malm et al., 2000; Debell et al., 2006; Hand et al., 2011). The version II sampler began operating in November 1999 through early 2000 and currently is in use at all IMPROVE sites. The version II sampler was implemented to allow for protocol changes that occurred in 2000 with the expansion of the IMPROVE network and the need for consistency with the EPA's fine mass and fine speciation monitoring network, specifically, the need for consistency with the EPA's sampling schedule. Other sampling configuration changes for IMPROVE occurred to ensure more-consistent data collection protocols (e.g., inlet height, filter collection time after sampling). Details regarding the version I sampler can be found in previous reports (e.g., Malm et al., 2000).

The IMPROVE samplers (versions I and II) consist of four independent modules (A, B, C, and D; see Figure 1.3). Each module incorporates a separate inlet, filter pack, and pump assembly. Modules A, B, and C are equipped with 2.5 µm cyclones that allow for sampling of particles with aerodynamic diameters less than 2.5 µm ($PM_{2.5}$), while module D is fitted with a PM_{10} inlet to collect particles with aerodynamic diameters less than 10 µm. Each module contains a filter substrate specific to the analysis planned (Figure 1.3).

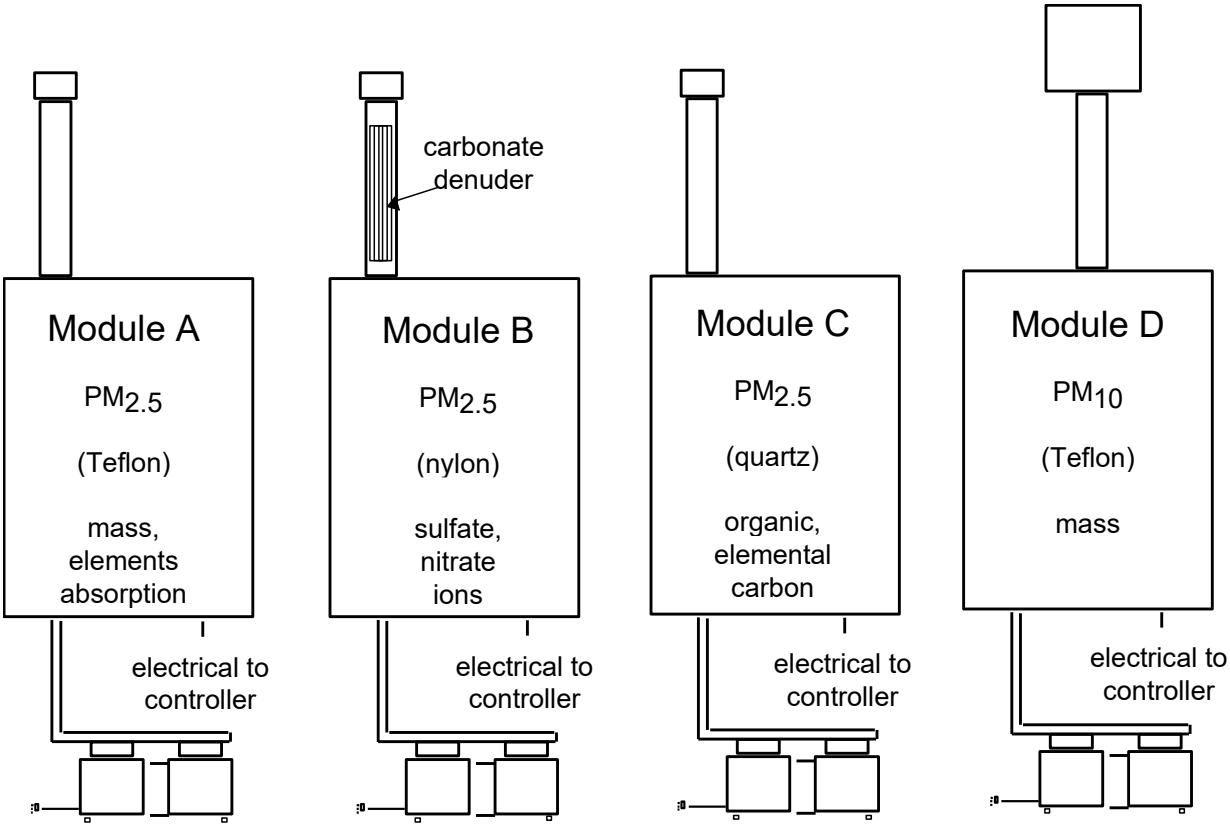

Figure 1.3. IMPROVE sampler showing the four modules with separate inlets and pumps. Substrates with analyses performed for each module are also shown.

To accommodate the every-third-day sampling schedule, the version II sampler has a four-filter manifold for each module. The manifold with solenoid valves sits directly above the

filter cassettes and is raised or lowered as a unit to unload and load the filters. The four filter cassettes are held in a cartridge (shown in Figure 1.4) that is designed to allow only one orientation in the sampler. Date- and site-labeled filter cartridges, along with memory cards, are sent from the analysis laboratory to the site and are returned in special mailing containers. If filter change service is performed on a sample day, the site operator moves the cassette containing that day's filter to the open position in the newly loaded cartridge. The few minutes that it takes to perform this sample change is recorded by the microprocessor on the memory card so that the correct air volume is used to calculate concentrations.

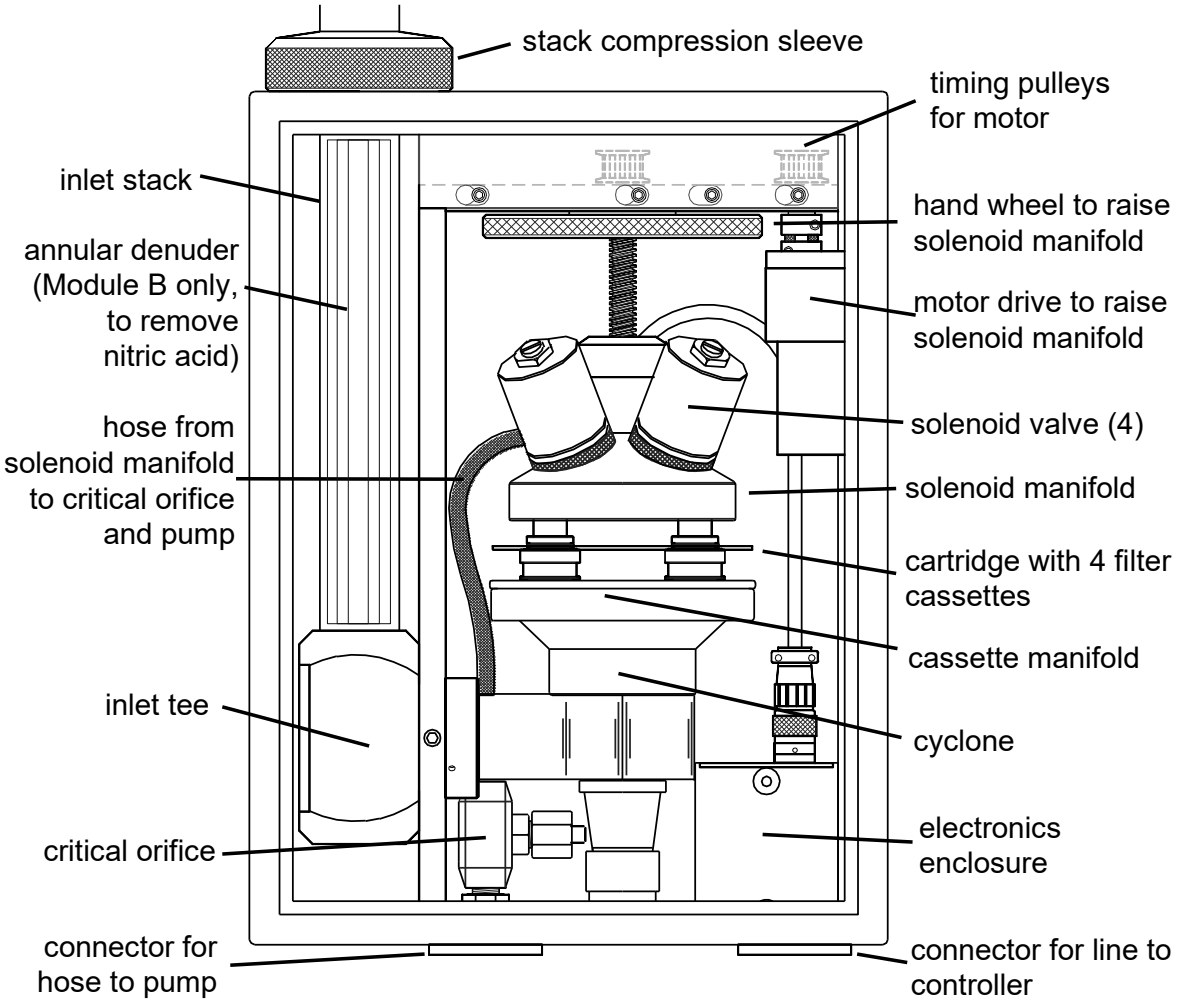

Figure 1.4. Version II IMPROVE sampler $PM_{2.5}$ module.

The version II sampler electronics became obsolete around 2011, and thus it became harder to maintain, repair, and obtain replacement parts. In 2018 and 2019, the version II sampler electronics were upgraded throughout the network and are referred to as version 4. The version 4 controller uses a Beaglebone Black development platform along with custom-designed electronics boards to manage all the sampler operations. The version 4 controller also includes an LCD color display that provides comprehensive instructions on how to operate the sampler, including diagrams and videos to assist the operator. Flow rate, sample temperature, and other operating parameters are recorded throughout the sample period on a secure digital (SD) card. In

addition, the data are uploaded to the University of California, Davis (UC Davis),[1] on a nightly basis. Internet connections using mobile carriers or nearby Wi-Fi connections were established at all the sites when the new controllers were installed. The controllers can be accessed remotely to diagnose and troubleshoot problems, operate the hardware (e.g., turn on/off pumps, lower the sampling manifold, turn on/off solenoids), and upgrade the software. Data received from the sampler are reviewed on a daily basis, allowing equipment problems to be quickly identified and resolved. Several new software tools have been developed to process and display this new data stream.

At some IMPROVE sites, a fifth module is added to accommodate replicate sampling and analysis for mass and composition. This quality assurance module is operated for each sampling period and collects a replicate sample for one of the four modules so that, over time, relative precision information can be developed for each parameter. Starting in 2003, collocated modules were installed at 25 sites across the network, providing ~4% replication for each of the four modules. Sites with only one additional module include four collocated A modules, three collocated B modules, three collocated C modules, and two collocated D modules. In addition, the Phoenix site (PHOE5) has a complete collocated sampler with all four modules (Table 1.3).

[1] UC Davis is the National Park Service contractor during the period of this report.

Table 1.3. Sites with a fifth collocated module.

Site Name	Site	A	B	C	D	Date of Operation
Mesa Verde NP	MEVE1	X				08/13/2003-present
Olympic NP	OLYM1	X				11/08/2003-05/14/2013
Proctor Maple Research Facility	PMRF1	X				09/03/2003-present
Sac and Fox	SAFO1	X				11/20/2003-07/01/2011
St. Marks NWR	SAMA1	X				11/18/2004-present
Trapper Creek	TRCR1	X				06/22/2004-06/25/2013
Yosemite NP	YOSE1	X				10/24/2012-present
Big Bend NP	BIBE1		X			08/30/2003-05/20/2013
Blue Mounds	BLMO1		X			09/16/2004-present
Frostburg	FRRE1		X			04/15/2004-present
Gates of the Mountains	GAMO1		X			09/23/2003-05/14/2013
Lassen Volcanic NP	LAVO1		X			04/18/2003-05/14/2013
Mammoth Cave NP	MACA1		X			05/12/2003-present
San Gabriel	SAGA1		X			11/20/2018- present
Everglades NP	EVER1			X		07/11/2003-12/15/2017
Hercules-Glades	HEGL1			X		08/24/2004-present
Hoover	HOOV1			X		08/13/2003-05/14/2013
Medicine Lake	MELA1			X		09/25/2003-present
Saguaro West NP	SAWE1			X		03/25/2004-05/20/2013
Seney	SENE1			X		08/10/2003-05/14/2013
Everglades NP	EVER1			X		06/02/2003-present
Houston	HOUS1				X	04/30/2004-09/01/2005
Jarbidge WA	JARB1				X	06/30/2004-05/14/2013
Joshua Tree NP	JOSH1				X	08/07/2003-05/14/2013
Quabbin Summit	QURE1				X	09/04/2003-05/20/2013
Swanquarter	SWAN1				X	11/09/2004-present
Wind Cave NP	WICA1				X	09/17/2004-present
Breton	BRIS1				X	01/28/2008-05/20/2013
Phoenix	PHOE5	X	X	X	X	03/01/2004-present

NP = National Park
NWR = National Wildlife Refuge
WA = Wilderness Area

The laboratory at UC Davis prepares the sample cartridges for the IMPROVE sites. Every three weeks, UC Davis sends containers with the necessary sampling supplies to each site. The containers are typically received 10 days before the first sample-change day of the next three-week cycle. Often there will be two containers at a site, one in current use and the second ready for the next period or ready to be shipped back to UC Davis. The site operators send the container with the exposed filters back to UC Davis within one to two days following the completion of each three-week cycle. All shipments, to and from the field, are sent by second-day express delivery. Thus, a sample container typically spends a little over a month between shipment from and delivery to UC Davis, with the filters installed in the sampler during one week of that period.

As these filters arrive at UC Davis from the field sites, they are placed in Petri dishes and accumulate until a shipping tray has been filled, usually 400 filters. Nylon filters are sent to the Research Triangle Institute (RTI)[2] for ion analysis, and quartz filters are sent to the Desert

[2] RTI is the NPS contractor for the ion analyses during the period of this report.

Research Institute (DRI)[3] for carbon analysis. Full trays of each type are sent to RTI and DRI approximately once a week by overnight express.

Module A is equipped with a PTFE (polytetrafluoroethylene) Teflon® (referred to as "Teflon") filter that is analyzed for $PM_{2.5}$ gravimetric fine mass (also referred to as fine mass, FM), elemental analysis, and filter light absorption. Samples are pre- and post-weighed to gravimetrically determine $PM_{2.5}$ fine mass using an electro-microbalance, after equilibrating for four hours at 30–40% relative humidity (RH) and 20–30° C. This procedure for determining gravimetric fine mass is associated with both positive and negative artifacts. Negative artifacts include loss of semivolatile species such as ammonium nitrate (AN) and some organic species from the Teflon filter during sampling. Positive artifacts include particle-bound water associated with hygroscopic aerosol species such as sulfates, nitrates, sea salt, and some organic species. Reactions with atmospheric gases may also contribute to positive artifacts. Storage conditions and shipping conditions may also contribute to artifacts. Beginning with samples and field blanks collected in October 2018, the gravimetric measurements are performed in the Measurement Technology Laboratories (MTL) AH500E climate-controlled, automated weighing system. Modules A and D Teflon filters are weighed in the MTL chambers with strict environmental controls, with the temperature set to 21.5 ºC ± 1.0 ºC and RH set to 39% ± 2.0%.

Elemental analysis is performed on the module A Teflon filters for elements with atomic number greater than 11 (Na) and less than 82 (Pb) by X-ray florescence (XRF), with a subset of elements reported. The techniques used for elemental analysis for the IMPROVE network have included proton elastic scattering analysis (PESA), proton induced X-ray emission (PIXE), and XRF. Elemental hydrogen was quantified using PESA. PIXE was used for quantifying nearly all elements with atomic number greater than 11 and less than 82, although not all were reported. Beginning in 1992, however, analysis of heavier elements with atomic weights from 26 (Fe) to 82 (Pb) switched to XRF with a molybdenum (Mo) anode source. PIXE was discontinued in late 2001 and analysis of the lighter elements with atomic numbers from 11 (Na) to 25 (Mn) was changed from PIXE to XRF using a copper (Cu) anode source. Also, in late 2001, the analysis of Fe was changed from Mo anode XRF to Cu anode XRF. In both cases the change from PIXE to XRF provided lower minimum detection limits (MDLs) for most elements of interest, as well as better sample preservation for reanalysis. The exceptions were Na, Mg, Al, and to a lesser extent Si, where the change to Cu XRF resulted in significantly increased MDL and uncertainty. The details on the transitions from PIXE to XRF are provided in Section 1.3.1.3. Starting in 2011 the XRF analysis has been performed with Malvern PANalytical Epsilon 5 XRF instruments as described in Section 1.3.1.3.

Field blanks are collected to determine positive artifacts that are used to correct concentrations of all the reported elements. A field blank filter is placed in an unused port in the filter cassette where it is exposed to all aspects of the filter handling process, with the exception of sample air drawn being through it. Artifact corrections are performed by subtracting the median field blank from the same filter lot as that as of the sample filters. The field blank correction is specific to each filter lot, and a minimum of 35 field blanks are required for a median to be calculated, which may require including field blanks from the previous month (SOP 351 Data Processing and Validation, http://vista.cira.colostate.edu/Improve/particulate-

[3] DRI is the NPS contractor for the carbon analyses during the period of this report.

monitoring-network/). Figure 1.5 presents field blank values for elements measured with XRF from January 2019 to January 2020.

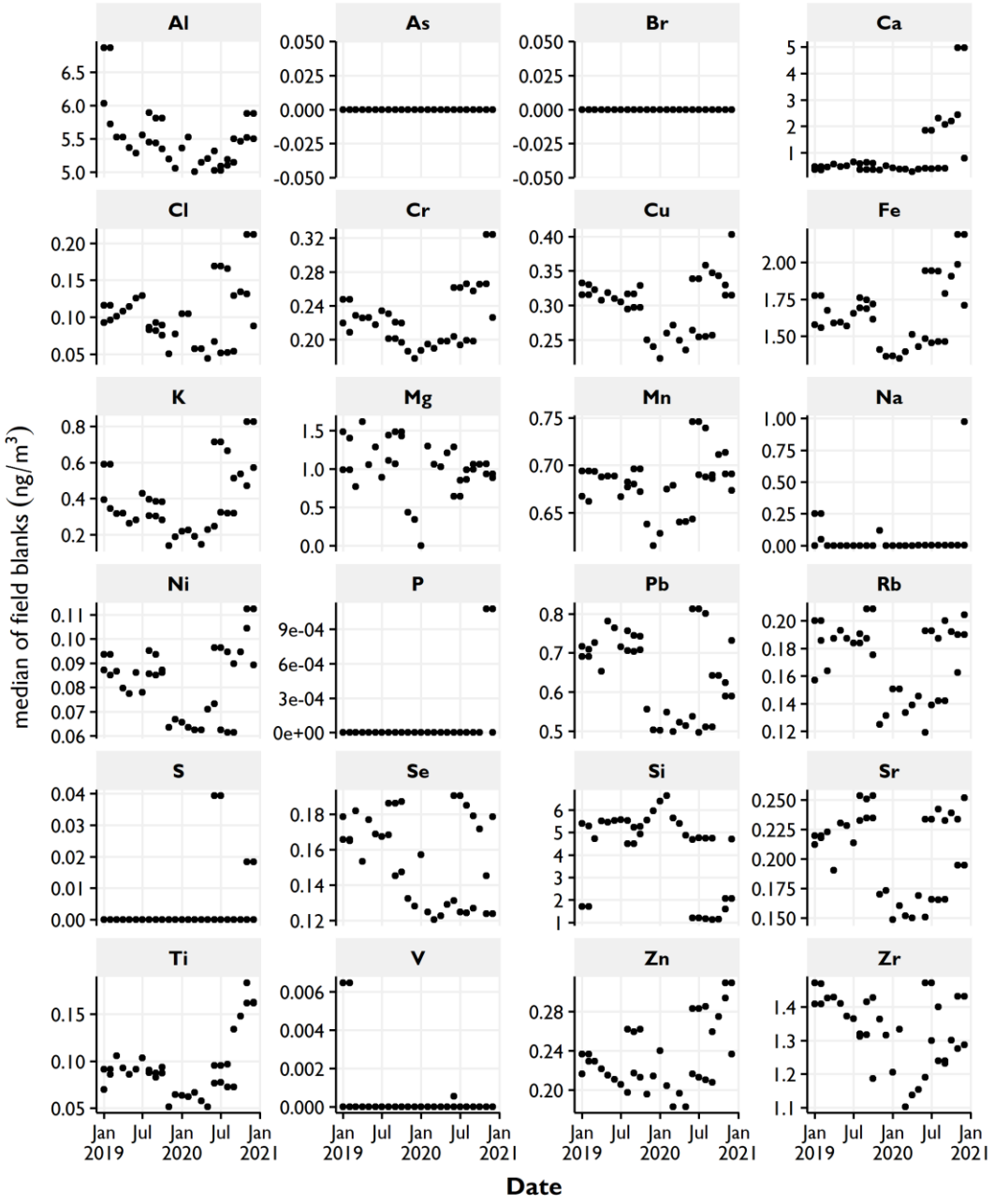

Figure 1.5. IMPROVE XRF field blank concentrations (ng m^{-3}) for elemental species from January 2019 to January 2021.

The filter light absorption coefficient (f_{abs}, Mm^{-1}) is determined from the channel A Teflon filter using a hybrid integrating plate/sphere system (HIPS) that shines a laser light (wavelength of 633 nm) on the backside of filter and measures reflected and transmitted light to determine the light absorption by the $PM_{2.5}$ sample. Field blank samples are used to calibrate the HIPS system to zero absorption. Prior to 1 March 1994, a laser integrating plate method (LIPM)

was used that did not include measurement of the reflection. Additional discussion of f_{abs} calibration is in Section 1.3.1.4.

Module B is fitted with a sodium carbonate denuder tube in the inlet to remove gaseous nitric acid in the air sample, followed by a Nylasorb (nylon) filter as the collection substrate. The material collected on the nylon filter is extracted ultrasonically in an aqueous solution that is subsequently analyzed for the anions sulfate, nitrate, nitrite, and chloride using ion chromatography (IC). The negative artifact associated with the loss of nitrate on Teflon filters is not as critical for nylon filters, as they have been shown to be more effective at capturing and retaining nitrate from semivolatile AN than Teflon filters (Yu et al., 2005).

Field blanks for the B module are collected to determine positive artifacts that are used to correct concentrations of all the reported anions. Field blanks are collected randomly at all sites on a periodic basis. When there are more than 50 field blanks in a month, the artifact is calculated as the median loading measured on the field blanks. Otherwise, values from the previous month are included until at least 50 field blanks are available. Artifact corrections are subtracted from ambient concentrations for the corresponding month. A single artifact correction is applied for each species for every site in the network for the period being processed. Monthly median field blanks for measured ions are shown in Figure 1.6 for 2016 through 2020.

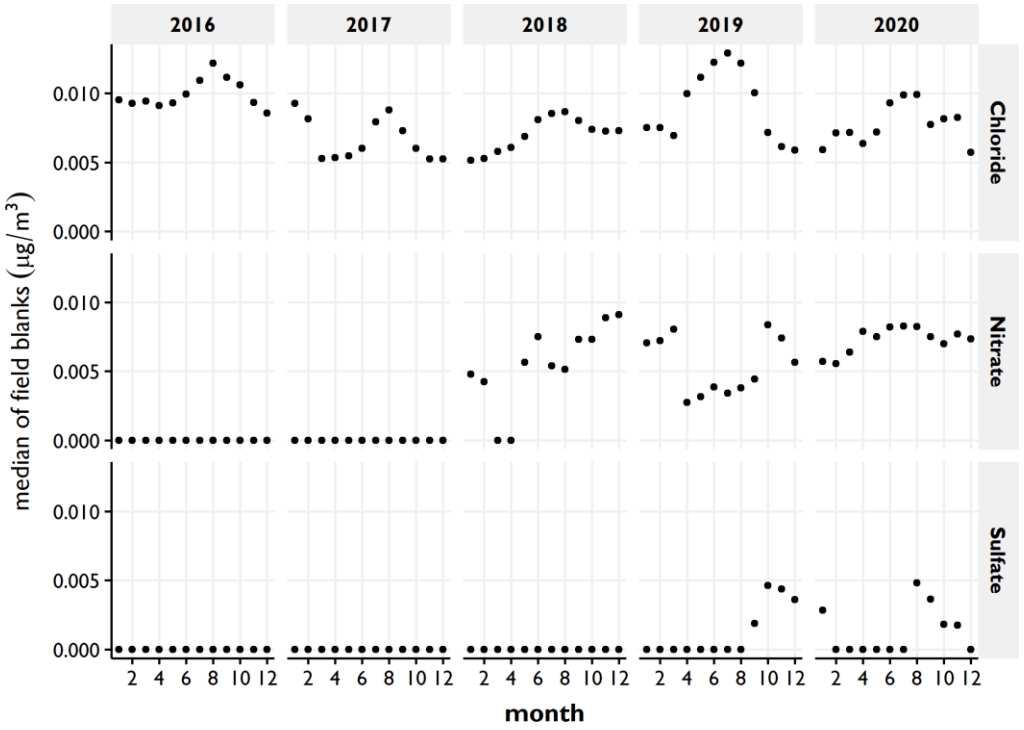

Figure 1.6. IMPROVE monthly median field blank concentrations (µg m^{-3}) for ions for 2016 through 2020.

Module C uses quartz fiber filters that are analyzed by thermal optical reflectance (TOR) for particulate organic and elemental carbon (OC and EC, respectively) (Chow et al., 1993). The fraction of carbonaceous aerosols evolving at high temperature during TOR is referred to in this report as "elemental carbon" following its operational definition and the recommendation by Petzold et al. (2013) that reflects the measurement technique and associated scientific literature.

However, “light absorbing carbon” is likely a more inclusive description of this carbonaceous aerosol fraction because particles evolving at high temperature may not be graphitic.

Thermally derived carbon fractions, including OC and EC, have been measured since 2016 using the DRI Model 2015 multiwavelength carbon analyzer (Chen et al., 2015; Chow et al., 2015a). As discussed in Section 1.3.1.1, measurements prior to this were made with different instruments, but equivalence among the carbon fractions was demonstrated by replicate measurements with the old and new instruments to assure long-term consistency. In this method, reflectance (R) from and transmittance (T) through a punch from the quartz filter are monitored continuously as the temperature is ramped through different steps that define the fractions. The evolved carbon at each temperature step is oxidized to carbon dioxide and quantified with a nondispersive infrared detector. R and T are monitored at 405, 445, 532, 635, 780, 808, and 980 nm wavelengths throughout the analysis to detect OC charring to EC of the aerosol deposit and organic vapors adsorbed throughout the quartz filter (Chow et al., 2001; Chow et al., 2004). Carbon that evolves after R returns to its initial value for the 635 nm wavelength in a 98% He/2% O_2 carrier gas is classified as EC in the aerosol deposit. EC by transmittance (ECT) is usually less than EC by reflectance (ECR), as T is dominated by the filter-adsorbed gases owing to charring of organic vapors adsorbed within the quartz-fiber filter (Chow et al., 2004; Chow et al., 2010; Watson et al., 2009). The amount of carbon associated with charring during the process is referred to as OP. When the reflected or transmitted light returns to its original intensity, the pyrolized (charred) OP is assumed to have been removed. Temperature-defined fractions are 1) OC1, OC2, OC3, and OC4 that evolve in a pure He [>99.999%] atmosphere at 140, 280, 480, and 580 °C, respectively; and 2) EC1, EC2, and EC3 that evolve in a 98% He/2% O_2 atmosphere at 580, 740, and 840 °C, respectively). The analysis temperature stays constant until each fraction is fully evolved, and total analysis times are longer for more heavily loaded samples. In addition to the carbon fractions, the following categories and their analytical uncertainties are reported: 1) total organic carbon by reflectance (OC; OC1 + OC2 + OC3 + OC4 + OP); 2) total elemental carbon by reflectance (EC; EC1 + EC2 + EC3 - OP); 3) total carbon (TC): all carbon evolved from the filter punch between ambient (~25 °C) and 840 °C during analysis; and 4) laser signals, including initial, minimum, and final laser reflectance and transmittance value counts for each wavelength. Analytical precisions for each batch of measurements are calculated from replicate analyses, MDLs are determined from laboratory blanks, and lower quantifiable limits (LQLs) are determined by the variability of passive field blanks (Watson et al., 2001).

Organic carbon concentrations reported by IMPROVE are corrected for an approximate positive artifact (Dillner et al., 2009). Positive artifact corrections account for contamination by the filter medium, handing the cassettes, or adsorption by gases during collection that are erroneously measured as particles. Field blanks are handled as normal filters (loaded into cassettes and cartridges, shipped to and from the field, and left in the sampler for a week) except no air is drawn through them. Field blanks are collected randomly at all sites on a periodic basis. When there are greater than 50 field blanks in a month, the artifact corrections are calculated as the monthly medians and subtracted from ambient concentrations for the corresponding month (IMPROVE Standard Operating Procedure #351, http://vista.cira.colostate.edu/Improve/particulate-monitoring-network/). Monthly median carbon fraction field blanks are shown in Figure 1.7 for 2016 through 2020.

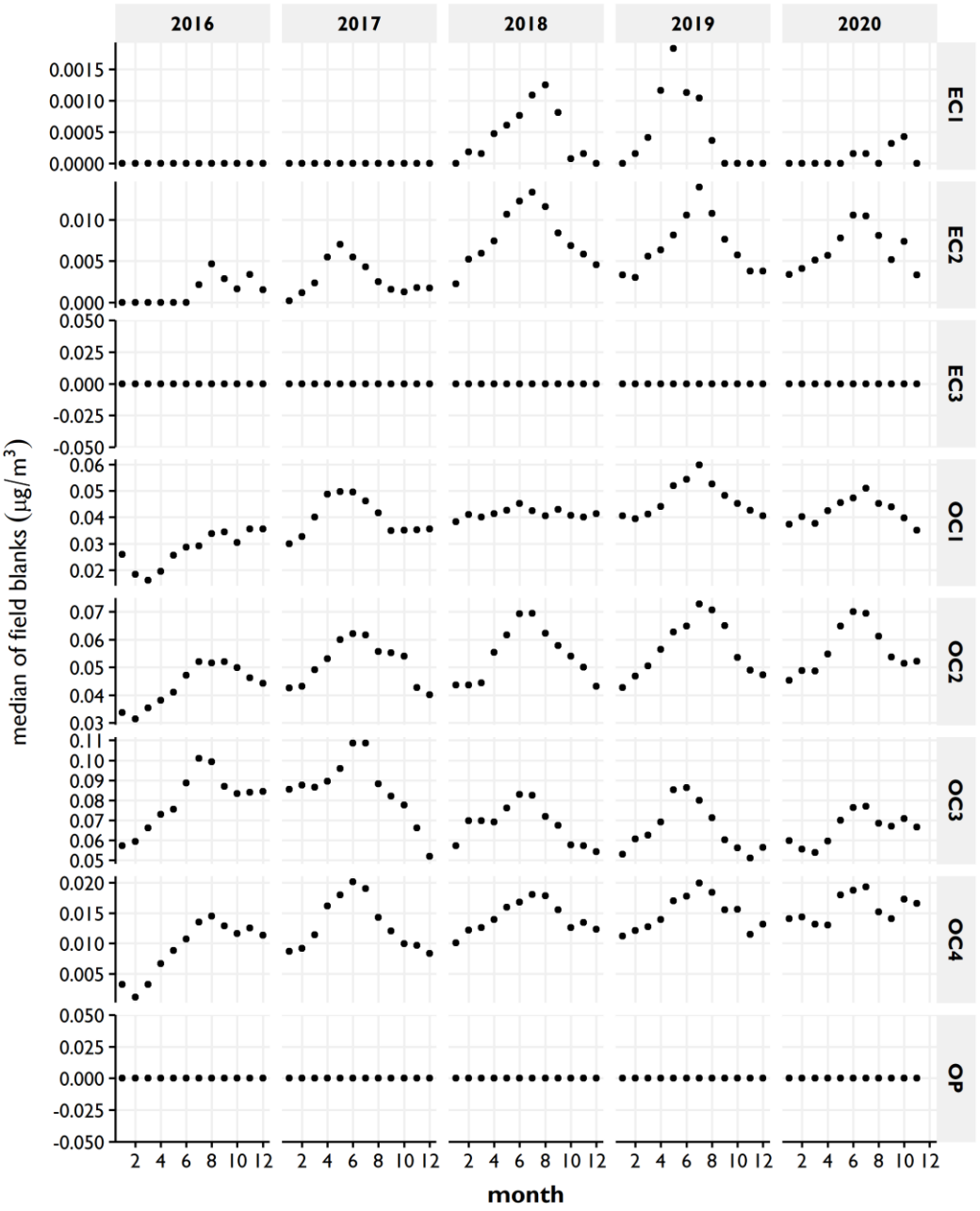

Figure 1.7. IMPROVE carbon fraction monthly median field blank concentrations (µg m^{-3}) from 2016 through 2020.

Negative artifacts due to the volatilization of particulate organics are not accounted for because they are thought to be small (Turpin et al., 2000), although some studies suggest they could be important. Changes in analytical methods due to hardware upgrades on 1 January 2005 resulted in changes in the split between OC and EC (Chow et al., 2007; White, 2007)). Higher EC/TC ratios were reported after the change in analytical methods, but no changes in TC were detected (White, 2007; see Section 1.3.1.1). Additional discussion of OC and EC concentrations can be found in Schichtel et al., 2021.

While OC and EC at 635 nm are used for estimating reconstructed mass (Chow et al., 2015b) and chemical extinction (Pitchford et al., 2007), the carbon fractions have been found useful for emissions characterization (Dewangan et al., 2016;Shibata et al., 2019), source apportionment (Kim and Hopke, 2004;Kim et al., 2004), and health studies (Wagner et al., 2014). The multiwavelength measurements are being used to determine the brown carbon (BrC) in source and ambient emissions and its effect on visibility and climate (Chen et al., 2021; Chow et al., 2018; Chow et al., 2021; June et al., 2020; Li et al., 2018; Shen et al., 2017).

Finally, module D is fitted with a PM_{10} inlet and uses a Teflon filter. PM_{10} aerosol mass concentrations are determined gravimetrically, following a similar protocol as $PM_{2.5}$ gravimetric mass measurements.

All IMPROVE data are available for download from the Federal Land Manager Environmental Database (FED: http://views.cira.colostate.edu/fed/).

All standard operating procedures (SOPs) are available online (https://airquality.ucdavis.edu/improve-documentation).

1.2.3 Optical Monitoring and Analysis

Routine optical monitoring includes light scattering coefficients as measured by nephelometers at a subset of IMPROVE monitoring sites. The number of nephelometer sites has decreased significantly due to budgetary constraints. Transmissometers, which were used to measure light extinction coefficients, are no longer operated at any IMPROVE site (Hand et al., 2011). Optical scenes are monitored using the NPS web camera network. A map of current nephelometer and web camera sites is shown in Figure 1.8.

Figure 1.8. Locations of nephelometers and web cameras.

The Optec NGN-2 open air nephelometer measures total ambient light scattering coefficients for all particles sizes at an effective wavelength of 550 nm (Molenar et al., 1989). The instrument's open-air design has minimal heating and allows a larger distribution of particle sizes to pass through it. It was designed with solid-state electronics that are very stable over a wide temperature and humidity range. It has an inherent limitation of an abbreviated acceptance angle in that it only samples light scattered between 5° and 175°, and the cut point of the instrument has not been characterized. Calibration of the instrument and data validation and processing algorithms are discussed in detail in Molenar and Malm (1992). Uncertainties in nephelometer calibration lead to multiplicative errors in measured scattering coefficients. Typical uncertainties for the Optec NGN-2 are on the order of 5–10% (Molenar and Malm, 1992).

During high humidity and precipitation events, the nephelometer can report erroneously high scattering coefficients. This is due to water condensing on the walls of the nephelometer and spray from raindrops impacting the screen on the nephelometer inlet. This water collects in the light trap and reflects light directly into the scattered-light detector, causing extremely high readings. In order to minimize this problem, the door of the nephelometer closes during heavy precipitation events, and a wick was added to the light trap to facilitate the removal of any collected water. A list of past and current nephelometer sites is provided in Table 1.4. Ten nephelometers are currently in operation. Data can be downloaded from the FED website (http://views.cira.colostate.edu/fed/).

Table 1.4. IMPROVE nephelometer network site locations.

Site	Code	State	Latitude	Longitude	Elevation (m)	Dates of Operation
Acadia NP	ACAD1	ME	44.38	-68.26	122	06/10/1993-12/01/1997
Acadia NP	ACAD2	ME	44.38	-68.26	157	04/01/1993-present
Big Bend NP	BIBE1	TX	29.30	-103.18	1067	01/01/1998-present
Bliss SP	BLIS1	CA	38.98	-120.11	2131	07/01/1996-03/31/2006
Boundary Waters Canoe Area WA	BOWA1	MN	47.95	-91.50	527	04/01/1993-12/31/1997
Brigantine NWR	BRIG1	NJ	39.47	-74.45	5	04/01/1993-06/30/1994
Cedar Bluff SP	CEBL1	KS	38.77	-99.76	666	07/01/2004-09/30/2007
Chiricahua NM	CHIR1	AZ	32.01	-109.39	243	10/01/2003-06/30/2010
Children's Park-Tucson	CHPA1	AZ	32.30	-110.98	704	04/01/2003-09/30/2010
Columbia River Gorge NSA	COGO2	WA	45.57	-122.21	243	04/01/2001-03/31/2005
Cohutta WA	COHU1	GA	34.79	-84.63	743	01/01/2004-03/31/2007
Columbia River Gorge NSA	CORI1	WA	45.66	-121.00	179	07/01/1993-03/31/2005
Tucson	CRAY1	AZ	32.20	-110.88	1707	01/01/2001-09/30/2010
Dolly Sods WA	DOSO1	WV	39.11	-79.43	1182	04/01/1993-12/31/2006
Phoenix	DYRT1	AZ	33.64	-112.34	364	07/01/2003-06/30/2016
Phoenix	ESTR1	AZ	33.38	-112.38	290	01/01/2003-06/30/2016
Gila WA	GICL1	NM	33.22	-108.24	1776	04/01/1994-12/31/2003
Glacier NP	GLAC2	MT	48.51	-114.00	939	10/01/2007-present
Great Basin NP	GRBA2	NV	39.01	-114.22	2066	01/01/2008-present
Grand Canyon NP	GRCA2	AZ	35.97	-111.98	2267	10/01/1997-present
Mount Baldy WA (Greer, AZ)	GRER1	AZ	34.07	-109.44	2513	04/01/2001-06/30/2010

Site	Code	State	Latitude	Longitude	Elevation (m)	Dates of Operation
Great Gulf WA	GRGU1	NH	44.31	-71.22	454	04/01/1995-03/31/2005
Great Smoky Mountains NP	GRSM1	TN	35.63	-83.94	811	04/01/1993-present
Green River Basin	GRVS1	WY	41.84	-109.61	1950	07/01/1996-12/31/2000
Pine Mountain WA (Humble Mountain)	HUMB1	AZ	33.98	-111.78	1586	01/01/1997-12/31/2003
Mazatzal WA (Ike's Backbone)	IKBA1	AZ	34.34	-111.68	1298	04/01/2001-06/30/2010
Grand Canyon NP (Indian Gardens)	INGA1	AZ	36.08	-112.13	1166	04/01/2004-09/30/2013
Jarbidge WA	JARB1	NV	41.89	-115.43	1869	04/01/1993-12/31/1997
James River Face WA	JARI1	VA	37.63	-79.51	290	10/01/2000-12/31/2003
Lone Peak WA	LOPE1	UT	40.44	-111.71	1768	10/01/1993-09/30/2001
South Lake Tahoe	LTBV1	CA	38.95	-119.96	1902	01/01/1996-09/30/2004
South Lake Tahoe	LTBV2	CA	38.93	-119.96	1904	10/01/2005-03/31/2006
Lye Brook WA	LYBR1	VT	43.15	-73.13	1015	07/01/1993-12/31/2003
Mammoth Cave NP	MACA1	KY	37.13	-86.15	235	01/01/1993-present
Mayville	MAYV1	WI	43.44	-88.53	306	10/01/2000-12/31/2006
Mazatzal WA	MAZA1	AZ	33.91	-111.43	2164	01/01/1997-09/30/2000
Sierra Ancha WA (McFadden Peak)	MCFD1	AZ	34.0	-111.0	2175	10/01/1997-03/31/2000
Milwaukee	MILW1	WI	43.00	-87.89	193	04/01/2004-06/30/2006
Mount Rainier NP	MORA1	WA	46.76	-122.12	439	01/01/1993-present
Mount Zirkel WA	MOZI2	CO	40.54	-106.68	3243	10/01/1993-09/30/2009
Galiuro WA (Muleshoe Ranch)	MUSR1	AZ	32.35	-110.23	1402	07/01/1997-06/30/2005
National Capitol - Central	NACA1	DC	38.9	-77.04	514	04/01/2003-03/31/2016
Nebraska National Forest	NEBR1	NE	41.89	-100.34	883	07/01/2005-09/30/2007
Okefenokee NWR	OKEF1	GA	30.74	-82.13	48	01/01/1993-06/30/1997
Organ Pipe NM	ORPI1	AZ	31.95	-112.80	366	04/01/2003-06/30/2010
Petrified Forest NP	PEFO3	AZ	34.91	-109.8	1690	10/01/2003-06/30/2010
Phoenix	PHON1	AZ	33.50	-112.10	372	04/01/1997-06/30/2018
Quaker City	QUAK1	OH	39.94	-81.34	372	04/01/2002-03/31/2004
Superstition WA (Queen Valley)	QUVA1	AZ	33.29	-111.29	668	04/01/2003-06/30/2010
Cape Romain NWR	ROMA1	SC	32.94	-79.66	5	01/01/2004-12/31/2012
Rocky Mountain NP	ROMO3	CO	40.28	-105.55	2760	01/01/2008-present
Chiricahua WA (Rucard Canyon)	RUCA1	AZ	31.78	-109.30	1637	10/01/1997-06/30/2001
Seney NWR	SENY1	MI	46.29	-85.95	216	01/01/2002-06/30/2006
Shenandoah NP	SHEN1	VA	38.52	-78.43	1079	07/01/1996-present
Shining Rock WA	SHRO1	NC	35.39	-82.77	1617	04/01/1994-09/30/1999
Sierra Ancha WA	SIAN1	AZ	34.09	-110.94	1600	07/01/2000-06/30/2010
Alpine Lakes WA	SNPA1	WA	47.42	-121.43	1049	07/01/1993-06/30/2001
Sycamore Canyon WA	SYCA1	AZ	35.14	-111.97	2046	07/01/1998-06/30/2010
Three Sisters WA	THSI1	OR	44.29	-122.04	885	07/01/1993-present
Tucson	TUCN1	AZ	32.24	-110.96	745	04/01/1997-06/30/2001
Saguaro NP (Tucson Mountain)	TUMO1	AZ	32.28	-111.17	754	10/01/1996-12/31/2001

Site	Code	State	Latitude	Longitude	Elevation (m)	Dates of Operation
Saguaro NP (Tucson Mountain)	TUMO2	AZ	32.25	-111.22	754	10/01/2001-06/30/2010
Upper Buffalo WA	UPBU1	AR	35.83	-93.20	722	01/01/1993-09/30/2009
Phoenix (Vehicle Emissions)	VEIX1	AZ	33.46	-112.00	345	04/01/2003-06/30/2016
Virgin Islands NP	VIIS1	VI	18.34	-64.80	51	04/23/1998-09/30/2005
Wichita Mountains NWR	WIMO1	OK	34.73	-98.71	509	07/01/2004-09/30/2007

NM = National Monument
NP = National Park
NWR = National Wildlife Refuge
NSA = National Scenic Area
SP = State Park
WA = Wilderness Area

Monitoring of scenic views is accomplished using digital cameras to document the visual impact of regional and layered hazes as a function of aerosol concentrations. Scene monitoring has the added benefit of displaying real-time park imagery to the public through the NPS Air Resources Division (ARD) website (https://www.nps.gov/subjects/air/webcams.htm). Images are provided in two sizes, and archived images are available online (https://www.nps.gov/AirWebCams/). Scene monitoring is more in line with the simple definition of visibility; scene characteristics include observer visual range, scene contrast, color, texture, and clarity and have the distinction that they are also dependent on scene and lighting conditions.

Early scene monitoring was accomplished using automated 35-mm camera systems. At each camera site, a spectrum of images associated with varying haze levels have been digitized and are available from the IMPROVE website (http://vista.cira.colostate.edu/IMPROVE/). These early camera systems have been replaced with webcams that take still photographs and upload images to the NPS Air Resources Division web page every 15 minutes at 22 locations in national parks across the country (https://www.nps.gov/features/ard/webcams/webcams.htm). A list of currently operated webcams is provided in Table 1.5.

Table 1.5 Web camera network site locations.

Site	Code	Latitude	Longitude	Elevation (m)	Start Date
Acadia NP	ACAD	44.38	-68.26	158	06/1/1999
Big Bend NP	BIBE	29.33	-103.21	1170	08/1/2001
Bryce Canyon NP	BRCA	37.48	-112.24	2766	09/1/2013
Denali NP	DENA	63.47	-150.84	694	07/1/2004
Dinosaur NM	DINO	40.44	-109.31	1549	10/31/2018
Grand Canyon NP	GRCA	36.06	-112.12	2150	11/1/2001
Great Smoky Mountains NP - Clingmans Dome	GRSM-CD	35.56	-83.50	1935	05/1/2018
Great Smoky Mountains NP - Look Rock	GRSM-LR	35.63	-83.94	793	04/1/1998
Great Smoky Mountains NP - Purchase Knob	GRSM-PK	35.59	-83.07	1500	08/19/2003
Grand Teton NP	GRTE	43.67	-110.60	2307	08/30/2011
Hawaii Volcanoes NP	HAVO	19.43	-155.26	1213	01/6/2011

Site	Code	Latitude	Longitude	Elevation (m)	Start Date
Joshua Tree NP	JOTR	34.00	-116.00	1265	11/1/2001
Mammoth Cave NP	MACA	37.19	-86.10	226	12/1/2001
Mount Rainier NP	MORA	46.79	-121.73	1650	07/1/2003
National Capital NMMP	NACA	38.89	-77.07	60	07/1/2003
North Cascades NP	NOCA	48.67	-121.27	163	07/16/2014
Olympic NP	OLYM	48.09	-123.80	191	07/1/2003
Point Reyes NS	PORE	38.00	-123.02	30	01/1/2004
Sequoia/Kings Canyon NP	SEKI	36.57	-118.78	1927	10/1/2002
Shenandoah NP	SHEN	38.62	-78.32	1015	01/19/2011
Theodore Roosevelt NP	THRO	46.90	-103.38	966	08/1/2002
Yosemite NP	YOSE	37.71	-119.71	1606	10/25/2005

NMMP = National Mall and Memorial Parks
NP = National Park
NM = National Monument
NS = National Seashore

1.3 PROTOCOL AND EQUIPMENT CHANGES

While consistency through time is critical to a monitoring program that tracks trends, significant changes in sampling, analysis, and data processing have occurred in the history of the IMPROVE network. Most of the changes were implemented to improve the quality or usefulness of the IMPROVE dataset or to increase the overall effectiveness of the network within available resources. Evaluations were conducted prior to many of the changes to assess and, where possible, identify approaches that would minimize the effects of changes on the dataset. In addition, IMPROVE routinely conducts data consistency assessments, specifically designed to identify and attempt to explain data discontinuities and trends that are not thought to be associated with changes in atmospheric conditions. The results of these assessments are used to inform decisions concerning the operation of IMPROVE and to alert data users via data advisories posted on the IMPROVE website. This section encompasses changes that have occurred since IMPROVE report V. Many of the summaries in this section reference data advisories on the IMPROVE website that provide additional information, including data plots and useful graphics (http://vista.cira.colostate.edu/Improve/data-advisories/).

1.3.1 Analytical Changes

1.3.1.1 Carbon Analyzer Replacements

OC and EC on quartz filters have been measured by DRI since 1987, starting with laboratory analyzers developed at the Oregon Graduate Institute (OGI, now part of the Oregon Health and Science University).

By the late 1990s it was evident that the DRI/OGC analyzers were deteriorating. Some components were no longer manufactured, and the data acquisition system was antiquated. The Model 2001 (Atmoslytic Inc., Calabasas, CA) analyzer was developed and made commercially available as a replacement. It introduced a number of enhancements, including better characterization of sample temperature and sample atmosphere, automatic sample positioning, more rapid temperature response, improved seals and flow control, greater heating capacity, advanced electronics, modern data acquisition, the potential for an automated sample changer,

and the ability to simultaneously measure reflectance and transmittance. Concurrent with the hardware modifications was the application of a new TOR protocol, named IMPROVE_A, designed to reflect the more accurate and less variable temperature and sample atmosphere conditions provided by the new instruments.

The Model 2001 analyzer was used for routine analysis of IMPROVE samples collected on or after 1 January 2005. Extensive testing prior to deployment had suggested that observable differences in the data record would be minimal (Chow et al., 2005). However, subsequent examination of data from the first two years of analysis (2005 and 2006) revealed unforeseen differences between data from the old and new instruments (White, 2007). The differences vary as a function of site, but the new data generally identify a higher proportion of TC as EC and a lower proportion as OC than were observed in the final years of the old instruments. The EC/OC distinction is operationally defined, and the differences are not fully understood (White, 2007).

Samples acquired after 1 January 2016 have been analyzed with the Model 2015 multiwavelength carbon analyzer (McGee Scientific Instruments, Berkeley, CA) as described in Section 1.2.2.

1.3.1.2 Environmentally Controlled Chamber Measurements of $PM_{2.5}$ and PM_{10} Gravimetric Mass

From December 2010 through September 2018, IMPROVE $PM_{2.5}$ and PM_{10} gravimetric mass measurements were performed manually in a temperature-controlled laboratory using Mettler-Toledo XP6 microbalances. Prior to 2011, periodic laboratory measurements suggested that RH was typically below 50%; however, a laboratory relocation in 2011 resulted in highly variable RH conditions in the weighing laboratory. Laboratory RH was not continuously recorded, but available data suggested that RH varied significantly during weighing and since 2011 exceeded 40% for almost half of the analyses, occasionally exceeding 60% (White, 2016). Thus, from 2011 to 2018, gravimetric mass data were potentially subject to high RH conditions and likely contained particle-bound water (Hand et al., 2019).

Beginning with samples and field blanks collected in October 2018, UC Davis transitioned from manual weighing to the Measurement Technology Laboratories (MTL) AH500E climate-controlled automated weighing system. The MTL AH500E system was used for the vast majority of the mass measurements from 2019 through 2020, although occasionally the system failed and the samples had to be weighed manually as shown in Figure 1.9.

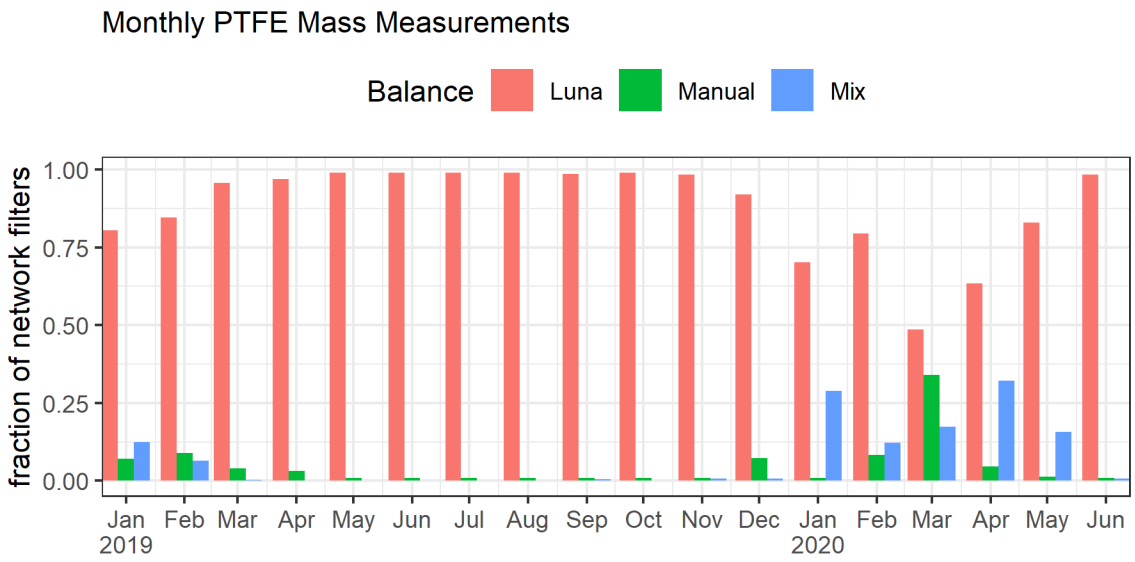

Figure 1.9. Fraction of IMPROVE network samples from January 2019 through June 2020 weighed on the MTL automated weighing system (Luna), the manual balance, or a mix of the two (e.g., pre-sampling mass from MTL automated weighing system and post-sampling mass from manual balance).

1.3.1.3 Transition from Custom-built XRF Instruments to PANalytical Epsilon 5 Instruments

A timeline of the elemental analysis methods employed at UC Davis is shown in Figure 1.10. PIXE analysis with the Crocker Nuclear Laboratory (CNL) cyclotron at UC Davis was originally used for all of the elements. From 1992 through 2010, IMPROVE samples were analyzed on two XRF instruments that employed copper (Cu) and molybdenum (Mo) X-ray sources, collectively referred to as the CuMo systems. These instruments were fabricated and used by CNL. The Cu XRF system initially operated in a helium environment, which simulates a vacuum photon path length with less sealing requirements. In 2005, the Cu XRF system was converted to vacuum to improve sensitivity for light elements. The Mo XRF system always operated in air since the interferences are low energy (e.g., argon Kα peak occurs at 2.96 KeV), and this instrument only quantified elements with an atomic number (Z) of 26 and higher (≥ 6.40 KeV). New XRF instruments (Malvern PANalytical Epsilon 5, abbreviated E5, Armelo, The Netherlands) were introduced for analysis of all IMPROVE samples starting 1 January 2011 to replace the aging systems.

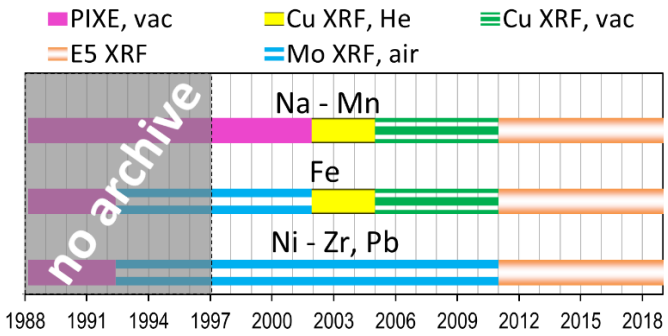

Figure 1.10. Timeline of elemental characterization methods used to analyze IMPROVE samples at UC Davis. PANalytical XRF is abbreviated "E5".

To evaluate the performance of these new instruments, archived IMPROVE filters were analyzed both on the Cu- and Mo-anode XRF instruments and the PANalytical Epsilon 5 (E5) instrument. The archived filters for Great Smoky Mountains NP (GRSM1), Point Reyes NS (PORE1), and Mount Rainier NP (MORA1) were retrieved and inspected. The filters from each site were then assembled into a queue for analysis on the same instruments. The Cu-anode XRF in vacuum was used for the light elements and the Mo-anode XRF in air was used for the heavier elements in 2011. A subset of the archived filters from GRSM1, PORE1, and MORA1 were analyzed on the E5 XRF instruments for comparison. Figure 1.11 shows the results from the two instruments; five elements (P, Cr, As, Sr, and Zr) were excluded due to low numbers of pairs above the detection limits. Clustering around the dashed 1:1 line is observed for all elements shown, indicating generally good agreement between the two measurements. However, deviations from this line are observed, particularly for low-Z elements (Na, Mg, Al, and Si) as well as the halogens Cl and Br as concentrations increase. Na, Mg, and Cl agree at lower concentrations but show distinct deviations in the 1:1 agreement at higher concentrations, with CuMo XRF reporting much higher concentrations than E5 XRF.

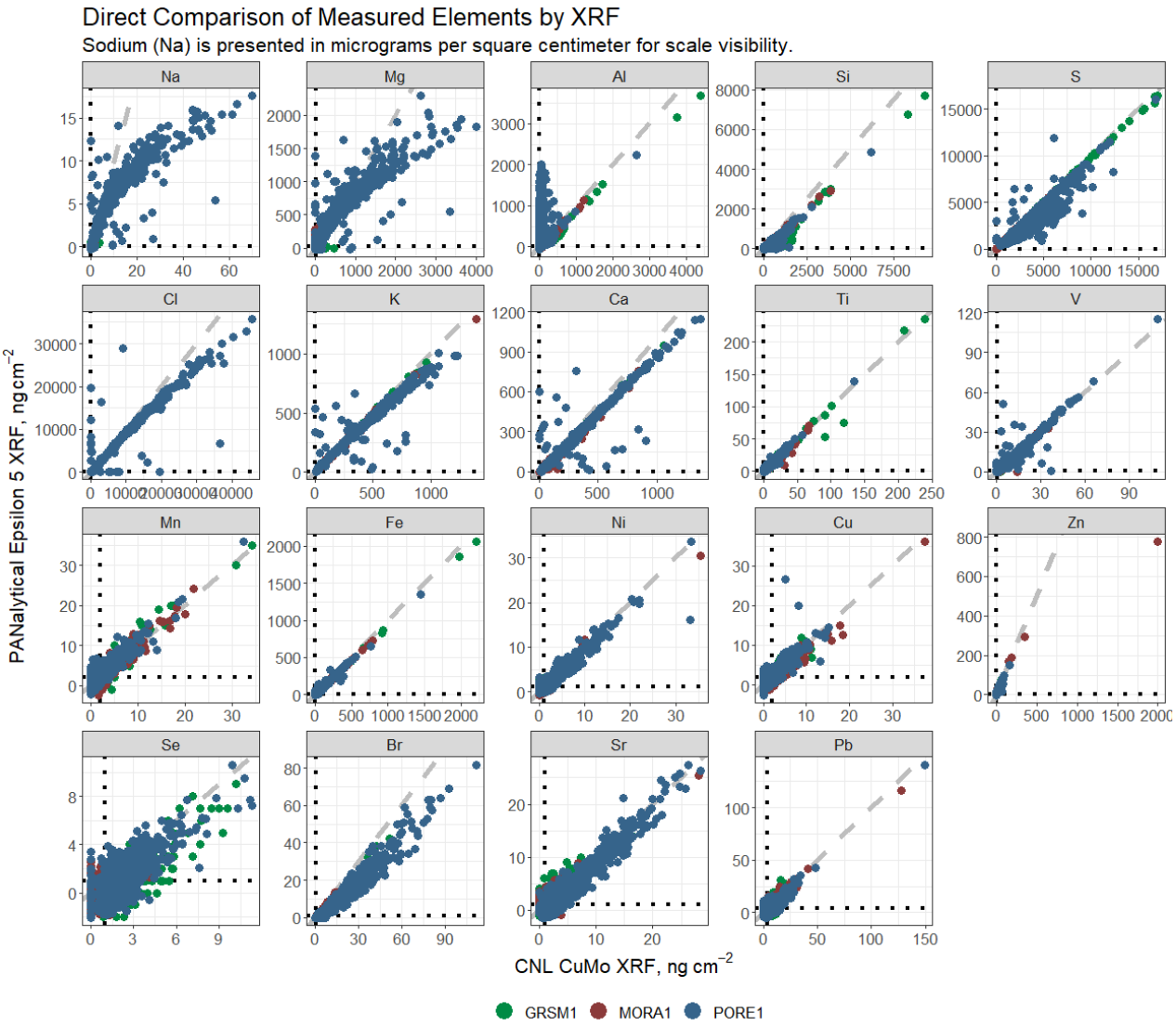

Figure 1.11. Scatterplots showing the agreement between XRF analytical instruments for elements routinely measured above 3 times the reported MDLs. Black dotted lines show the reported MDLs for each element and instrument while gray dashed lines show a 1:1 agreement, not a regression line. Data are for three sites (GRSM1, MORA1, and PORE1).

1.3.1.4 Changes to Filter Light Absorption Measurement (f_{abs})

Filter light absorption is quantified from HIPS measurements of transmittance (t) and reflectance (r) off the backside of a $PM_{2.5}$ Teflon filter since 1994. White et al. (2016) developed a calibration method based on fundamental principles where the HIPS t and r are calibrated such that $r + t = 1$ for clean filters. Unexposed field and lab blanks are used for the clean filters. Filter absorption (f_{abs}) is calculated with equation (1.1),

$$f_{abs} = \frac{f}{V} \times \tau_{abs} = \frac{f}{V} \ln\left(\frac{1-r}{t}\right) \qquad (1.1)$$

where f is the area of the sample deposit, V is the volume of air sampled, and τ_{abs} is the absorption optical depth. The f_{abs} measurements are not equivalent to ambient absorption (b_{abs}), due in part to the potential for changes in aerosol absorbing properties as they are deposited on the filter. Also, the illumination of the aerosol in the atmosphere is columnar, while the HIPS calibration model approximated the illumination as diffuse, which would yield twice the effective path length and resulting optical depth. Actual sample illumination is anisotropic and $1 \leq f_{abs}/b_{abs} \leq 2$. Calibrating the system to blank filters has the advantage that the system is demonstrably well calibrated at zero absorption and should not suffer from biases at low values. The measurement of both r and t accounts for changes in filter scattering properties. However, it was found that filters with significantly different light scattering properties require a separate calibration. Consequently, filter acceptance testing is important to ensure the calibration is applicable to a given filter batch. HIPS is not a fully calibrated system since reference standards with known absorbing properties are not used in the calibration. However, there has been adequate theoretical and empirical evidence for the linearity of the response of HIPS to absorbing particulate matter in lightly loaded samples (White et al., 2016). Retrospective analyses of 15 years of IMPROVE samples have demonstrated that HIPS f_{abs} measurements are stable and reproducible.

Multiple changes and updates have been made to the UC Davis HIPS system. In April 2018 the HIPS integrating sphere was changed from the legacy 2-inch Spectraflect-coated sphere described in White et al. (2016) to a newer 4-inch Spectralon sphere from the same manufacturer, and the laser was replaced. A calibration was performed following the April 2018 instrument upgrades; samples were analyzed under this calibration beginning with those collected January 2017. Additionally, in November 2018 new detectors were installed and the instrument was subsequently recalibrated; samples collected beginning March 2018 were analyzed under this calibration. The possible effects on the data due to modifications and new calibrations will be evaluated and reported in an upcoming data advisory.

Table 1.6. Changes and updates made to the UC Davis HIPS system.

Lab Date	Change	Reason	Comments
05/09/2017	HIPS moved to new laboratory	Instrument moved to new lab to help with environmental light and vibration issues.	
~10/1/2017	Change of the laser in the system.	The old HeNe laser lost power output and a new HeNe laser was purchased and installed.	New laser is Thor Labs model HNL050R, 5 mW 632.8 nm.
03/07/2018	Replacement of old 2-inch integrating sphere with newer 4-inch sphere.	Old sphere was dirty and it was thought better consistency would be gained with the larger sphere.	Old sphere was a 2-inch Labsphere Spectraflect model. The new sphere is a 4-inch Labsphere Spectralon model.
03/26/2018	Removed the black pipe between laser and integrating sphere.	The pipe was used to house a diffuser and optics which are no longer used. The assembly was removed to address light leakage and alignment issues.	

Lab Date	Change	Reason	Comments
8/24/2018	Replaced reflectance and transmittance detectors and their power meters.	Detectors were over 30 years old, and the transmittance detector was losing stability.	New power meter is a dual input Newport 2936-R. Reflectance detector is a Si photodiode with a built in OD 3 neutral density filter, Newport 918D-SL-OD3R. Transmittance detector is the same but with an OD2 filter, Newport 918D-SL-OD2R.
8/24/2018 – 10/22/2018	Tested various iterations of neutral density filters and diffusers for the integrating plate.	Old plate optics (neutral density filter and opal glass diffuser) did not fit the lens tube for the new transmittance detector. They were replaced with 2-inch optics which fit the new lens tube.	Final plate optics arrangement is a 0.6 OD neutral density filter at the end of the lens tube closest to the sample filter with an opal glass diffuser directly behind it. Both mounted on a 0.5-inch long, 2-inch diameter lens tube connected to the detector via a short adapter.
11/08/2018	Start routine use of new detectors and integrating plate.	Testing complete and routine sample analysis began.	

For sample dates from January 2003 through December 2016 (HIPS analysis dates prior to April 2017), HIPS data calibration and operation are as described in White et al. (2016). For sample dates from January 2017 through February 2018 (HIPS analysis dates 12 April 2018 to 17 August 2018), the data are reported with a new calibration that reflects the installation of the 4-inch sphere and removal of the diffuser tube assembly. For samples dates from March 2018 through present (HIPS analysis dates of 16 November 2018 to present), data are reported after recalibration for the new detectors and integrating plate optics.

In addition to the abovementioned changes, in April 2020, the control software for the HIPS instrument was upgraded from a combination of Excel macros and a data acquisition card to LabVIEW control software that pulls digital data directly off the new detector controller that was installed in November 2018. The new LabVIEW control software provides an intuitive user interface to the instrument and automates more of the measurement process including writing instrument results directly to the database.

1.3.1.5 Fourier Transform-Infrared Spectroscopy (FT-IR)

For the last decade, Fourier transform-infrared (FT-IR) spectroscopy has been explored to cost-effectively reproduce existing IMPROVE speciation data and to measure additional speciation data in the form of organic functional groups. FT-IR spectra are measured from IMPROVE $PM_{2.5}$ Teflon filters with a nondestructive 5-minute analysis per sample.

A multitude of compositional data can be obtained from FT-IR analysis because many aerosol constituents have bonds that absorb infrared light. Proof-of-concept work began with efforts to reproduce TOR OC and EC data at the seven collocated module A sites in 2011 (Dillner and Takahama, 2015a; Dillner and Takahama, 2015b) and were extended to 11 additional sites in 2013 (Reggente et al., 2016). A select group of spectra was calibrated to TOR OC and EC data to accurately predict FT-IR OC and EC concentrations in all other samples, as

long as the mass range and chemical composition of samples in the calibration set were similar to the samples to be measured. In addition, samples from one year were used to predict samples in another year. Analysis on multiple FT-IR instruments suggested that several instruments could be used interchangeably as long as environmental conditions for the filters and the instruments were maintained over time (Debus et al., 2019), resulting in calibration for all instruments rather than a single calibration for each instrument. Applying calibrations networkwide to measure FT-IR OC and EC includes the need for one calibration per constituent measured (e.g., TC = OC + EC) due to the large variability in samples across the network. For example, samples influenced by forest fires or prescribed burns and those more typical of rural samples may require different calibrations in order to reproduce OC and EC from TOR (Takahama et al., 2019). This calibration method is conceptually different from calibrations with laboratory standards. However, the complexities of the carbonaceous fraction are not rivaled by other constituents (ions and elements), and calibration to ambient standards analyzed continuously provides a robust means of spanning the mass loadings, composition, and interferents as well as predicting operationally defined constituents for which there are no agreed upon standards.

Using networkwide data from 2015 through 2017, calibration methods and measurements of FT-IR OC, EC, and TC as well as inorganic ions (sulfate and nitrate) and dust elements (Si, Al, Ca, Ti, Fe), light absorption, and $PM_{2.5}$ mass were made for all continental U.S. sites (Debus et al., submitted). FT-IR measured concentrations were compared to routine IMPROVE data for all constituents. Reliably predicted concentrations were obtained for a broad range of atmospheric constituents with detectable infrared signatures such as OC, EC, TC, sulfate, dust elements, light absorption, and $PM_{2.5}$ mass. Due to volatilization off the Teflon filter, nitrate measurements were found to be unsatisfactory. To make this procedure operationally practical, select IMPROVE sites were used for calibration and the remainder of the sites were predicted using FT-IR spectra. The calibration sites were selected to represent the diversity of $PM_{2.5}$ concentrations and composition across the IMPROVE network. Strengths of the method include that it has nondestructive analysis, it has no gas-phase adsorption onto the Teflon filter (sampling artifact), it provides a new data stream of functional groups and most of the current suite of composition data, and it has a lower cost. Limitations of the FT-IR analysis include the use of the inconsistent Teflon filters with variable scattering and absorption that interferes with some peaks useful for measuring carbonaceous components, the lack of strong and unique absorptions related to EC, and the complexity of the spectra requiring advanced mathematical tools. A detailed description of FT-IR analysis, studies, and results can be found in Appendix 1.1.

1.3.1.6 Summary of Data Advisories

Data advisories are regularly posted to the IMPROVE website to inform users about events or measurement interferences that might affect the data (http://vista.cira.colostate.edu/Improve/data-advisories/). These events include both intentional and unintentional changes to instrumentation, procedures, or sampling media. Summaries of the data advisories that affected all sites were posted from 2011 through 2021 and are listed below.

- *Changes in Data Redelivery of 1/2005 through 5/2014 Data*
  Several changes were applied to the data from January 2005 through May 2014. Data downloaded before 20 April 2015 may not have these changes applied. The data advisory describes several changes, including carbon concentrations, MDLs, and uncertainties;

HIPS measurements, MDLs, and uncertainties; ion MDLs and uncertainties; updated flow rates; updated sample status flags; and XRF concentrations, MDLs, and uncertainties (Cheng, 2015).

- *Change to OC Artifact Correction Method for OC Carbon Fractions*
  OC carbon fractions are artifact-corrected to account for gas-phase adsorption of OC onto quartz filters. For data downloaded before May 2015, OC fractions were artifact-corrected using monthly median OC fractions from back-up quartz filters, located downstream the primary quartz filter at a few sites. The revised artifact correction method utilizes the monthly median blank filters collected at a few sites in the network. Blank filters have no air pulled through them but are loaded in the filter cassette and remain in the sampler for the same length of time as the sample filters (~7 days) (Dillner, 2015).

- *Change in Reporting of Filter Light Absorption*
  Light absorption by the module A Teflon filter has been monitored using a He-Ne laser operating at 633 nm. From 1988 through February 1994, filters were analyzed with a LIPM method. Samples collected since March 1994 have been analyzed with HIPS. In 2015 the HIPS calibration was improved and data were reprocessed back to 2003. The revised data are identified as f_{abs} (White, 2015a).

- *Bias in Masked and Unmasked Filter Light Absorption Measurements*
  Masks were historically used at many sites to reduce the collection area of module A filters from 3.53 cm^2 to 2.20 cm^2. As recently as 2003, masks were employed at approximately half of all sites; by the end of 2007, all masks were removed. An inequivalence in f_{abs} was noted between masked and unmasked samples (White, 2015b).

- *Increased Variation of Humidity in the Weighing Laboratory*
  IMPROVE gravimetric measurements have never been in compliance with EPA requirements regarding Federal Reference Method (FRM) determination of $PM_{2.5}$ mass. Starting with samples in 2011, IMPROVE filter handling and weighing operations were relocated to a different laboratory at UC Davis. The new laboratory did not have regulated RH capabilities. Additional analyses suggested that $PM_{2.5}$ gravimetric mass could be influenced by particle-bound water associated with hygroscopic species on the filters, especially during periods with higher laboratory RH (White, 2016; Hand et al., 2019).

- *Negative Chloride Concentrations at Salt-poor Sites*
  At coastal sites influenced by marine aerosols, the module B chloride ion measurement has been indicative of fresh sea salt. Chloride is a less reliable tracer farther inland due to atmospheric reactions that deplete it. From 2000 through 2003, samples at many interior sites were associated with strictly negative concentrations. These negative concentrations were due to excessive chloride backgrounds on 37-mm nylon filters used during that period. This problem was addressed by switching suppliers of nylon filters with much lower backgrounds for 2004 and onward (White, 2017a).

- *Over-reporting of Sodium in Salt-rich Samples*
  Elemental concentrations in samples analyzed with the legacy PIXE and XRF systems were reported with a semi-empirical correction for the attenuation of X-rays within the sample deposit. Attenuation increases as the element's atomic number decreases and is

strongest for Na, the lightest element reported. Samples collected since the beginning of 2011 have been analyzed with the Episilon 5 PANalytical XRF. Results from this system do not include an adjustment for sample thickness (White, 2017b).

- *Calibration Bias in Reported Vanadium Concentrations*
  Elemental concentrations from XRF analysis are based on linear calibrations of the instruments. Since the 2011 sample year, two thin-film standards certified by a commercial manufacturer have underpinned the vanadium (V) calibration. These standards were returned in 2017 to the original manufacturer for recertification. The V loadings reported in 2017 were lower than previously certified values by a factor of about 1/1.3. The XRF systems have been recalibrated using the newly certified V loadings of the same two original standards. The updated calibration yields XRF values consistent with quoted loadings for four new V standards purchased from the same manufacturer in 2017. V concentrations in samples collected starting in November 2017 are being reported with the new XRF calibration. Retrospective application of the 2017 recalibration back to 2011 assumes that the standards themselves did not change between their 2011 and 2017 certifications, and annual calibration records provide evidence of this stability (Trzepla, 2018).

- *Correction of Chloride Concentrations for Filter Blank Levels*
  This data advisory serves as an update on a 2009 data advisory (White, 2009). Elevated chloride mass loadings on nylon filter field blanks were observed between mid-2007 and early 2011. During this period, chloride blank values started climbing within the consumption of a single manufacturing lot, the reason for which was later found to be adsorption by unsampled nylon filters from their packaging. The problem was eliminated by new storage procedures for the next manufacturing lot, introduced with the February 2011 samples. To account for the elevated and varying chloride blank values, monthly blank correction was implemented in 2009 and applied retroactively to the post-2005 ion data. Later analyses, reported in a 2017 data advisory, suggest that unknown and variable portions of the contaminant (blank) chloride initially present in affected filters may have been lost during the subsequent active sampling. The blank corrections made to sample values may thus have been excessive; consistent with this hypothesis, recent analysis of chloride long-term trends revealed a small step increase in network-median ambient chloride concentrations when the improved storage procedures eliminated most of the contamination. Thus, it is advisable to use the chloride ion data between mid-2007 and early 2011 with caution (Zhang, 2019).

- *Updated Data for Carbon*
  Starting with January 2016 sample dates, DRI switched from Model 2001 to Model 2015 carbon analyzers for module C quartz filters. The Model 2015 analyzers directly measure carbon dioxide with a nondispersive infrared (NDIR) detector, where the earlier Model 2001 analyzers directly measured methane with a flame ionization detector (FID). Following quality assurance analyses, DRI determined that the software's initial threshold for peak integration was not appropriate for the new NDIR carbon signal. Carbon data from 2016 and early 2017 were reprocessed and redelivered (Schichtel, 2019).

- *Changes to HIPS System*
  The HIPS instrument for measuring light absorption was completely refurbished in 2018. Details are provided in the data advisory (Trzepla and Giacomo, 2019).

- *Method Change for Calibrating Flow Rate Transfer Standards*
  The flow calibration procedure prior to 2014 was creating a bias in the sampler flow rate calibrations, which led to low nominal flow rates at the IMPROVE sites. In November 2014, the method for calibrating each transfer standard against a primary standard was adjusted to avoid placing the two devices in series. A range of flowrates are now generated using a standard IMPROVE controller with a calibration cartridge that includes four different flow restrictions and are measured with 1) only the primary standard placed at the inlet to establish the reference flow rates and 2) only the transfer standard at the inlet. The calibration is now performed with three different calibration cartridges for a 12-point calibration, whereas the old calibration was only performed at four flow rates set using a needle valve. Evaluation of system pressure at the ORI (Open on Rise of Inlet) pressure tap indicated a negligible change in flow when switching between the two configurations. A comparison of transfer standard calibrations using the new method to previous calibrations of the same devices using the old method of devices in series shows that the new method results in a transfer standard calibration that is typically 2–3% lower on average at nominal sampler flow. The direction of this shift is consistent with expectations from the change in calibration method (Wallis, 2019a).

- *Change in Analytical Protocol for XRF Analysis*
  The element content of collected IMPROVE samples is quantified by energy-dispersive X-ray fluorescence (EDXRF) analysis. The PANalytical Epsilon 5 instruments used since the 2011 sample year employ a primary X-ray tube to excite a sequence of secondary targets, whose secondary excitation spectra in turn irradiate the sample. In order to improve detection of lead and some other elements, the analytical protocol for XRF analysis was slightly modified starting with samples collected in October 2018. The KBr secondary target, previously included to highlight arsenic, was dropped to allow more time for some of the other targets in the sequence. Longer target irradiation generally improves sensitivities for the elements reported from that target. The effects on data quality are expected to be small, detectable only after a sufficient record has been acquired with the new protocol. The XRF analyzers have now been recalibrated with the modified protocol, and all IMPROVE samples starting October 2018 are being reported with the new calibration and new analytical protocol (Trzepla, 2019).

- *Universal Calibration Constants for Flow Rate Calculation*
  In the past, the flow-rate calibration constants needed to be both site- and module-specific because the controller's pressure transducers were not calibrated to measure pressure in absolute units. Improvements in electronics now allow the use of universal constants for the entire network. The version 4 electronics are digital, and the pressure transducers provide absolute measures of pressure in inches of water for the cyclone transducer and pounds per square inch absolute (PSIA) for the orifice transducer. Quality control testing prior to deployment shows that the transducers are very consistent, with a full-scale, best-fit, straight-line accuracy of 0.25% and a maximum total error band of $\pm$2% full scale. Therefore, universal flow rate constants were implemented throughout the network. In 2018 and 2019, field calibrations from the 128 IMPROVE sites equipped with version 4

electronics were used to determine universal flow rate constants for the $PM_{2.5}$ and PM_{10} modules. The universal constants determined are intended to characterize the entire network, provided that standard equipment is used at each site. Flow constants will not change with each site maintenance visit; rather, equipment will be checked during maintenance to ensure that flow calculation is within specifications. If outside of specifications, the maintenance team will seek to determine the cause of the discrepancy and make repairs as necessary (Wallis, 2019b).

1.3.1.7 Quality Assurance Reports

Both UC Davis and RTI routinely review quality assurance (QA) activities, and reports are delivered semiannually (http://vista.cira.colostate.edu/Improve/quality-assurance/). The UC Davis report summarizes laboratory and data quality issues as well as analytical and data processing changes during the review period. The primary objectives of the report series are to

- provide graphics illustrating some of the comparisons used to evaluate the quality and consistency of measurements within the network;
- highlight observations that may give early indications of emerging trends, whether in atmospheric composition or measurement quality; and
- serve as a record and tool for ongoing QA efforts.

1.3.2 Sampling Equipment Changes

1.3.2.1 New Sampler Controller

UC Davis has developed new sampler controllers (V4 controller) and is currently updating new Ebox firmware to version 1.3. As of 30 June 2020, V4 controllers had been installed at all IMPROVE sites across the network in the United States and Canada. As of the same date, internet connections to all IMPROVE sites had been established except for Simeonof (SIME1) in Alaska and Baengnyeong Island (BYIS1) in South Korea. Sites with V4 controllers and internet connections are monitored in real time by UC Davis technicians, allowing faster follow up and recovery in cases where samples are being lost or equipment has failed.

1.3.2.2 Teflon Manufacturer Change

Beginning with samples and field blanks collected mid-October 2018, UC Davis transitioned to using Teflon filters made by MTL (Measurement Technology Laboratories) instead of Pall Corporation. Teflon filter field blanks from the A-module ($PM_{2.5}$; Figure 1.12) and D-module (PM_{10}; Figure 1.13) were gravimetrically analyzed to monitor contamination levels and balance stability. As seen in Figure 1.12 and Figure 1.13, there was a step increase in $PM_{2.5}$ and PM_{10} concentrations, respectively, measured from field blanks corresponding with the transition, indicating that the filters gained mass between pre- and post-weight measurements. Experiments conducted confirmed that the mass gain was connected to the filters themselves, not the weighing chamber. It was unclear what part of the filters was gaining mass (either the filter ring or the Teflon film) and if the gain was from water or potentially volatile organic carbon. UC Davis has continued working with both Pall Corporation and MTL to acquire Teflon filters that meet all quality specifications.

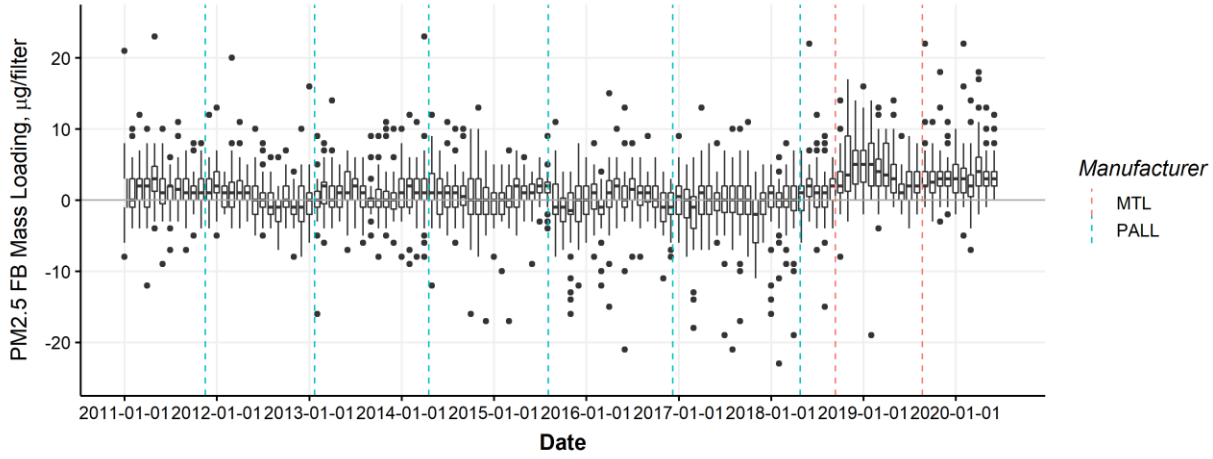

Figure 1.12. Time series of $PM_{2.5}$ (µg/filter) on Teflon filter field blanks (1 January 2011 through 30 June 2020). Blue vertical lines indicate manufacturer lot transition, where Pall Corporation is the manufacturer. Red vertical line indicates manufacturer transition to Measurement Technology Laboratories (MTL) as manufacturer.

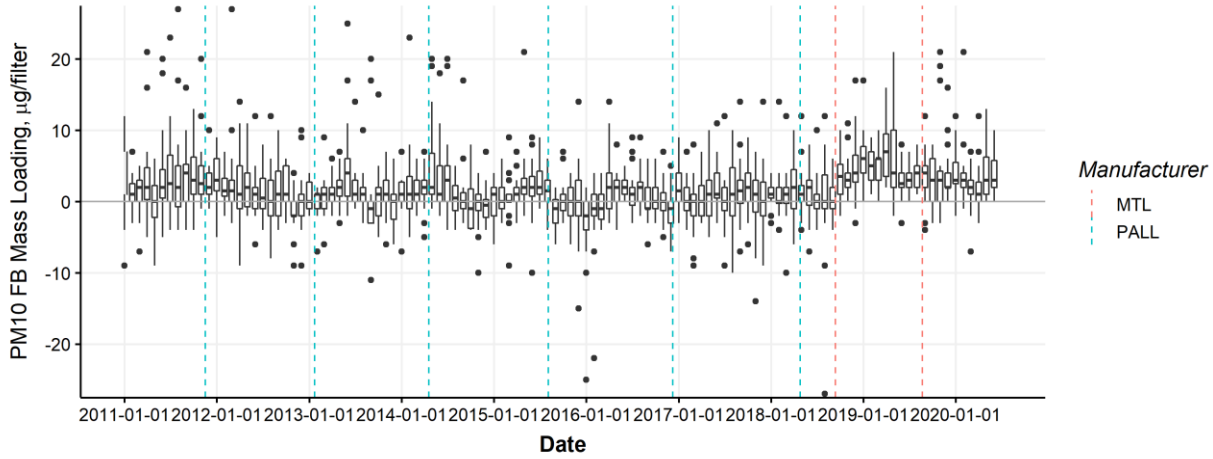

Figure 1.13. Time series of PM_{10} (µg/filter) on Teflon filter field blanks (1 January 2011 through 30 June 2020). Blue vertical lines indicate manufacturer lot transition, where Pall Corporation is the manufacturer. Red vertical line indicates manufacturer transition to Measurement Technology Laboratories (MTL) as manufacturer.

1.3.3 Data Processing Changes

During 2018 through 2020, IMPROVE data processing was modified to standardize field blank processing, uncertainty calculation, and MDL calculation across all analyses: gravimetric mass, XRF, IC, and thermal optical analysis (TOA) for OC and EC. Field blanks are used to calculate representative networkwide statistics that are used to perform artifact correction, estimate uncertainty, and calculate MDL. Prior to this period, the particulars of these estimates varied by analysis. There are now two standard calculation paths, one that is filter lot specific for analyses that are more dependent on filter lot variability and one that is independent of filter lot.

The lot-specific analyses are XRF and HIPS, while gravimetric mass, IC, and TOA are lot independent.

Artifact correction and MDL estimates are based on monthly field blank statistics, and reported uncertainty depends partly on the MDL estimate. For lot-independent analyses, a minimum of 50 field blanks is required to calculate the statistics, and a minimum of 35 field blanks is required for lot-specific analyses. In most cases, there are enough field blanks of each lot within a month to meet these minimum requirements. However, if there are not, the algorithm includes field blanks from prior and/or subsequent months until the minimum threshold is reached. The two statistics calculated are median and 95th percentile.

Concentrations are calculated with equation (1.2), where C is the ambient concentration (ng/m^3) and A is the mass measured on the filter (ng). The artifact mass, B (ng), is the field blank median for IC, TOA, and XRF, and zero for gravimetric mass and HIPS. The sample of air volume is given as V (m^3).

$$C = \frac{A-B}{V} \quad (1.2)$$

The reported MDL (ng/m^3) is calculated with equation (1.3):

$$MDL = \frac{max(P95-B, MDL_a)}{V} \quad (1.3)$$

where P95 is the 95th percentile of field blank mass (ng) and MDL_a is the analytical MDL determined and reported by the laboratory (ng). Concentration uncertainty ($\sigma(c)$, ng/m^3) is calculated with equation (1.4),

$$\sigma(c) = \sqrt{[fC]^2 + \left[\frac{0.608 * \max(P95-B, MDL_a)}{V}\right]^2} \quad (1.4)$$

where f is the fractional uncertainty. This term results from various sources of proportional uncertainties, such as analytical calibration and flow-rate measurements. Beginning with data from samples collected in January 2018, f is determined using the most recent two years of data from collocated measurements. If the count of collocated pairs over the two-year period is less than 60, a value of 0.25 is adopted as f.

The standardization of these calculations occurred in stages, outlined below.

- January 2018: Updated IC and TOA MDL

  Prior to sample day 1 January 2018, IC and TOA species MDLs were calculated using 3 × the standard deviation of each field blank set, rather than the 95th percentile now used. For most months, these calculations are similar; however, high outliers can make the standard deviation calculation significantly higher. This can occur, for example, when an intended field blank is accidentally sampled. The switch to 95th percentile provides a more stable estimate of MDL that is more robust against outliers. In addition, prior to sample day 1 January 2018, IC and TOA field blank statistics required a minimum of

three monthly field blanks instead of the 50 now required. There are routinely >50 field blanks each month, so this change has little impact.

- October 2018: Updated XRF processing

  The IMPROVE program uses three PANalytical Epsilon 5 XRF instruments. Prior to October 2018, XRF field blank analyses were aggregated by instrument used and instrument analysis date. There was no check to see if the field blanks were from the same sample collection period as the samples. As of October 2018, field blanks are aggregated using the universal methods described above, independent of instrument and separated by filter lot. This timing coincides with the change in analytical protocol described in the Section 1.3.1.6.

- January 2019: Update gravimetric mass and HIPS MDL

  Prior to data collected 1 January 2019, gravimetric mass and HIPS absorption were assigned static MDL values. Assuming nominal flow, the resultant reported MDLs were approximately 300 ng/m^3 for $PM_{2.5}$ mass, 400 ng/m^3 for PM_{10} mass, and 0.35 Mm^{-1} for filter absorption. As of January 2019 sample data, MDLs for all these parameters are calculated using the universal methods described above.

1.3.4 Summary of Changes

A summary of changes to the network since 2011 is listed in Table 1.7.

Table 1.7. Major network wide changes in sampling, analysis, and data reporting affecting samples collected January 2011 and later.

Change Date	Change Description
01/01/2011 (sampling date)	Introduced PANalytical XRF instruments for element analysis
02/01/2011	Transitioned from Cahn Microbalances to Mettler Toledo XP6 Microbalances
10/01/2012	New loose-screen sample cassettes deployed in network
09/29/2014	New sample handling laboratory software system deployed
11/01/2014	Changed method for calibrating flow rate transfer standards
01/01/2015	HIPS light absorption data (f_{abs}) between 2003 and 2015 reprocessed using new 2015 calibration and updated in FED database
04/20/2015	Changed duration criteria for clogged and clogging filters during redelivery of 1/2005-5/2014 data
04/20/2015	Changed temperature equation used in flow rate calculation during redelivery of 01/01/2005-05/01/2014 data
04/20/2015	Changed OC artifact correction from using back-up quartz filters to using monthly median blanks during redelivery of 1/2005-5/2014 data
2015-2016	Installed precision ruby orifices in PM_{10} modules to improve flow rate measurement
01/01/2016 (sampling date)	TOA carbon analysis transitioned from using DRI 2001 carbon analyzer to DRI 2015 multi-wavelength carbon analyzer
08/31/2017	Started delivery of IMPROVE semi-annual QA report
2018-2019	Deployed new sampler controller (V4 controller) including new Ebox with digital pressure transducers and internet connectivity throughout the network

Change Date	Change Description
01/01/2018 (sampling date)	Changed flow rate calculation to using universal flow constants for sites with V4 sampler controlled installed
10/01/2018 (sampling date)	Teflon filter manufacturer changed from Pall to MTL
10/01/2018	Modified XRF analytical application by removing KBr secondary target to improve sensitivity for selected elements
10/01/2018 (sampling date)	Introduced MTL weighing chamber for gravimetric analysis
2017	Implemented multiple changes to the HIPS system and data processing for filter light absorption measurement
2018	Standardized blank processing and MDL estimation for XRF, HIPS, gravimetric, IC and TOA analysis
02/01/2021 (deployment date)	Second MTL weighing chamber deployed. Mettler Toledo balance in both MTL weighing chambers upgraded to XPR6UD5 ultrabalances

1.3.5 IMPROVE Technical System Audits

Technical System Audits (TSA) of field operations are conducted to assess whether the IMPROVE sampling sites are in compliance with the IMPROVE Quality Assurance Project Plan (QAPP, http://vista.cira.colostate.edu/improve/wp-content/uploads/2020/02/IMPROVE-QAPP-Signed_3_2016_updated.pdf). TSAs focus primarily on evaluating the sampling sites and the particle samplers in the field. In conducting a TSA, the auditor

1. assesses whether the sampling site meets siting criteria for an IMPROVE sampler;
2. evaluates the integrity of the sampling structure;
3. checks the flow rate of each sampling module using a NIST (National Institute of Standards and Technology) certified flow meter;
4. observes the technique of the site operator (when possible);
5. asks the site operator to complete a questionnaire to ensure that (s)he has adequate sampler and sample change knowledge, that all safety concerns have been addressed, and that the current IMPROVE Operations Contractor is providing adequate support to run the sites.

From 2016 through 2022 nearly all of the IMPROVE sites have been audited, with the goal to complete TSAs at all sites within a ten year period. Figure 1.14 shows the locations of IMPROVE sites, with the symbol color denoting whether the site has been audited. Minor problems discovered during the audits are addressed by the Operation Contractor (currently UC Davis); major problems are addressed by a joint committee, including the principal investigator of the Operations Contractor, the Steering Committee Chair, and the contracting officer representative at NPS. Audit results are provided in annual TSA reports (http://vista.cira.colostate.edu/Improve/technical-system-audits/).

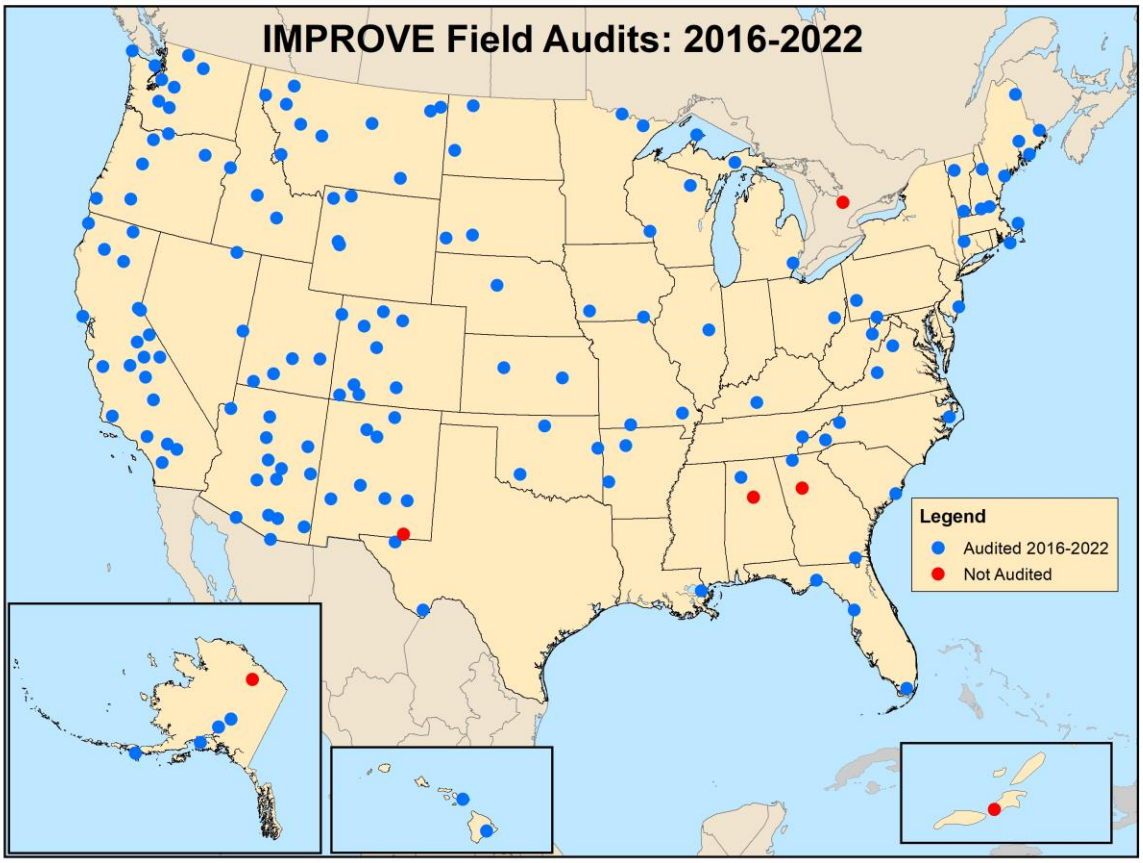

Figure 1.14 IMPROVE field site audits from 2016-2022. Blue symbols correspond to audited sites; red symbols are sites yet to have a technical system audit.

1.4 CHEMICAL SPECIATION NETWORK

The objectives of the EPA's Chemical Speciation Network (CSN) are to track progress of emission reduction strategies through the characterization of trends, validation of air quality modeling and source apportionment activities, and support of health effects and exposure studies. The CSN comprises approximately nearly 150 sites operated by state, local, and tribal agencies, primarily in urban/suburban settings.

The EPA's $PM_{2.5}$ speciation program was established in 1997 as a complement to the $PM_{2.5}$ Federal Reference Method (FRM) mass network. The pilot phase of the program included thirteen sites that operated from February through July 2000. The Speciated Trends Network (now referred to as the CSN) was deployed in the fall of 2000 (EPA, 2004). Historically, the CSN utilized several types of samplers, including the Thermo Andersen RAAS, Met One SASS, and the URG MASS (Solomon et al., 2014). The specific sampler employed at a given site was chosen by the state, local, or tribal agency. Currently, each site operates two samplers: a Met One SASS or SuperSASS for collection of Teflon (for elemental concentration using XRF) or nylon filters for ion concentration using IC. A URG 3000N sampler is used for collection of quartz filters for TOA. All samplers use a $PM_{2.5}$ inlet. Samplers operate on a 24-hour schedule from

midnight to midnight every third or every sixth day, and data are reported at local conditions. A detailed description of network operation and sampling details is provided in Solomon et al. (2014). In 2014, budget considerations led to changes in CSN operations, resulting in the elimination of the $PM_{2.5}$ mass measurement and defunding of 38 sites. Sample frequency was also reduced from every third day to every sixth day at a small number of CSN sites (https://ha.battelle.org/CSNAssessment/html/Default.html).

Historically, the RTI International Laboratory held the EPA CSN contract for filter shipping, handling, laboratory analysis (except for carbon analysis, which was subcontracted to DRI in 2007), and data reporting. In November 2015 the laboratory analysis and data processing activities were awarded to UC Davis, with ion and carbon analysis subcontracted to DRI. The filter shipping and handling was awarded separately to Wood PLC. A number of shifts in laboratory analysis and data processing methods also occurred. XRF laboratory analysis shifted from RTI to UC Davis starting with 20 November 2015 samples. IC laboratory analysis was subcontracted to DRI and then to RTI after 1 October 2018. Carbon laboratory analysis switched to UC Davis on 1 October 2018. A number of other changes occurred to methods for determining and applying blank corrections and reporting data with these contract changes; these are discussed in detail in the CSN data advisory in Appendix 1.2.

CSN carbon analysis was historically performed using thermal optical transmittance (TOT) using a NIOSH (National Institute for Occupational Safety and Health)-type protocol. The recognition that IMPROVE samplers and TOR analysis produce different OC and EC concentrations than CSN samplers and TOT analysis motivated the CSN transition to TOR analysis for consistency with the IMPROVE network and to the URG 3000N sampler. The conversion began in May 2007 with 56 sites, followed by another 63 sites in April 2009 and 78 additional sites in October 2009 (EPA, 2009). A discussion of the adjustments applied to CSN carbon data collected prior to the transition to the new analyses and monitors is provided by Malm et al. (2011). After 2009, carbon data from CSN and the IMPROVE network should be directly comparable, with the exception of blank corrections.

Starting 20 November 2015, concentration data for ions and carbon are reported with blank corrections (positive sampling artifacts). Prior to this date, only elements were blank corrected using filter lot-specific background levels. For samples collected between 20 November 2015 and 31 January 2017, elemental measurements were corrected using the laboratory filter blank median areal density from each manufacturer filter lot. Beginning in February 2017, elemental blank corrections used the monthly median of field blanks, consistent with other corrections. Blank corrections for ion data began with samples collected in January 2016, using monthly median data for the corresponding sample month. Carbon blank corrections are applied for each thermal subfraction of the thermal optical analysis, using the corresponding median value from the quartz field blanks during the sample month. Both corrected and uncorrected carbon data are reported to EPA's Air Quality System (AQS) database.

A map of 372 current and discontinued CSN sites is provided in Figure 1.15, with the general regions depicted. Twenty-nine regions for the CSN sites were empirically defined based on seasonal distribution of aerosol concentrations and site locations (Hand et al., 2011; Hand et al., 2012). For comparison purposes, sites were grouped into similar regions to those defined for the IMPROVE network. Of the 29 regions, eleven had only one site per region. A list of the 136

sites that met the completeness criteria (outlined in Chapter 2) is provided in Table 1.8, including site location, region, and setting (urban, suburban, or rural). The sites used in this report are shown as orange circles in Figure 1.15. CSN data can be downloaded from http://views.cira.colostate.edu/fed/ or http://www.epa.gov/ttn/airs/airsaqs/.

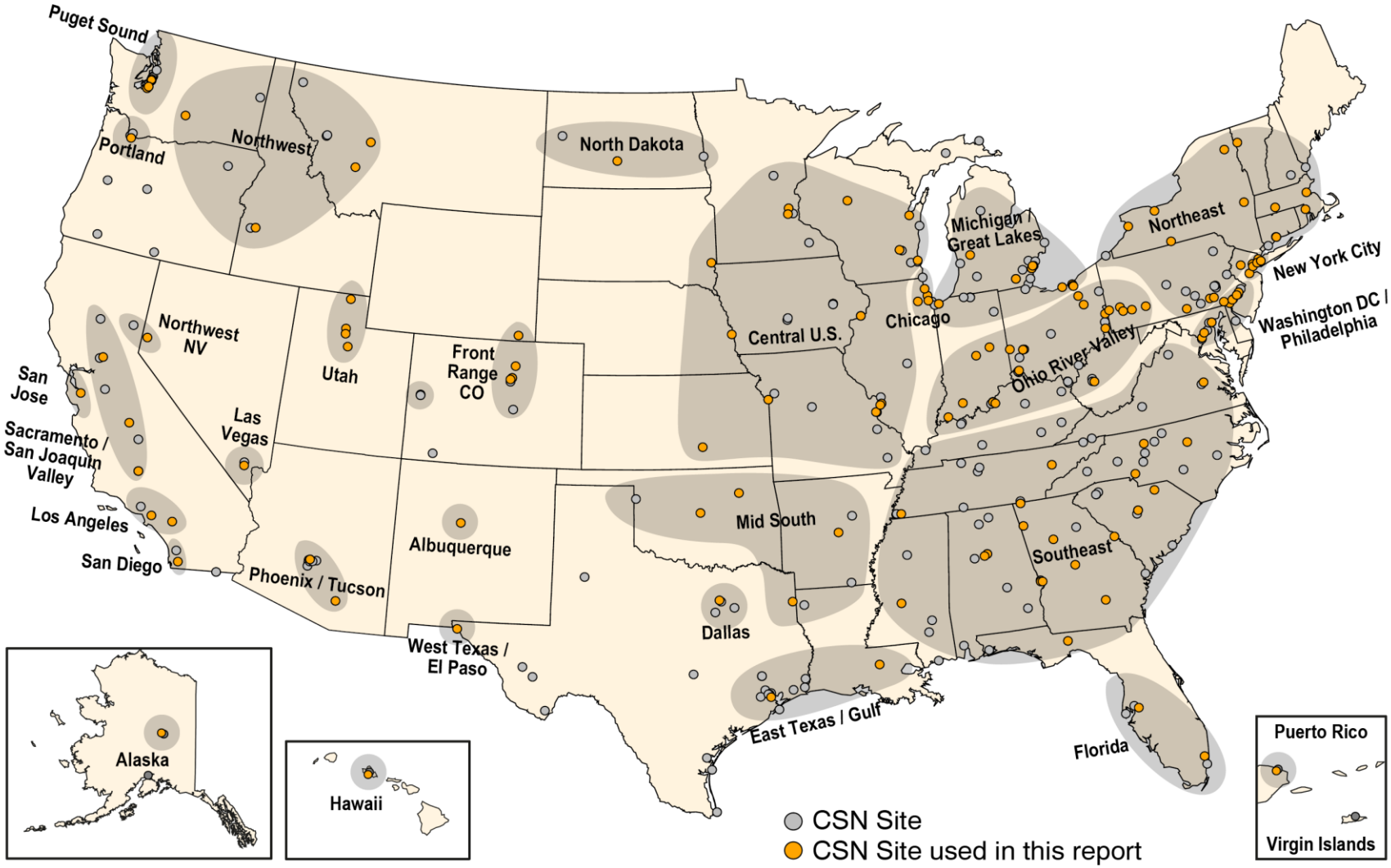

Figure 1.15. Current and discontinued Chemical Speciation Network (CSN) sites operated by the Environmental Protection Agency. Regions are shown as shaded areas and bold text. Sites included in the analyses in this report are shown as orange circles.

Table 1.8. Chemical Speciation Network (CSN) site location, elevation, setting and region.

Site	City	State	Region	Latitude	Longitude	Elevation (m)	Setting
				(deg)	(deg)		
10730023	Birmingham	AL	Southeast	33.553	-86.815	177	urban
10732003	Birmingham	AL	Southeast	33.5	-86.924	180	suburban
11130003	Phenix City	AL	Southeast	32.437	-84.999	25	urban
20900034	Fairbanks/NCORE	AK	Alaska	64.846	-147.727	132	urban
40139997	Phoenix	AZ	Phoenix/Tucson	33.504	-112.095	355	urban
40191028	Tucson	AZ	Phoenix/Tucson	32.295	-110.982	710	urban
51190007	Little Rock	AR	Midsouth	34.756	-92.276	77	urban
60190011	Fresno	CA	Sacramento/San Joaquin Valley	36.785	-119.773	96	suburban
60290014	Bakersfield	CA	Sacramento/San Joaquin Valley	35.356	-119.04	118	urban
60371103	Los Angeles	CA	Los Angeles	34.067	-118.227	126	urban
60658001	Rubidoux	CA	Los Angeles	34	-117.416	250	suburban
60670006	Sacramento	CA	Sacramento/San Joaquin Valley	38.614	-121.367	19	suburban
60731022	El Cajon	CA	San Diego	32.79	-116.944	141	suburban
60850005	San Jose	CA	San Francisco	37.349	-121.895	21	urban
80010008	Commerce City	CO	Front Range CO	39.828	-104.938	1574	urban
80310026	Denver	CO	Front Range CO	39.779	-105.005	1602	urban
81230008	Platteville	CO	Front Range CO	40.209	-104.823	1464	rural
90090027	New Haven	CT	Northeast	41.301	-72.903	5	urban
100032004	Wilmington	DE	Washington D.C./ Philadelphia Corridor	39.739	-75.558	31	urban
110010043	Washington D.C.	DC	Washington D.C./ Philadelphia Corridor	38.919	-77.013	31	suburban
120110034	Davie	FL	Florida	26.054	-80.257	2	suburban
120573002	Valrico	FL	Florida	27.966	-82.23	28	rural
120730012	Tallahassee	FL	East Texas/Gulf	30.44	-84.348	16	suburban
130210007	Macon	GA	Southeast	32.777	-83.641	103	suburban
130690002	Douglas	GA	Southeast	31.513	-82.75	64	rural
130890002	Panthersville	GA	Southeast	33.688	-84.29	244	suburban
131150003	Rome	GA	Southeast	34.261	-85.323	196	suburban
132150011	Columbus	GA	Southeast	32.431	-84.932	78	suburban
132450091	Augusta	GA	Southeast	33.434	-82.022	57	suburban
132950002	Rossville	GA	Southeast	34.978	-85.301	200	suburban
150030010	Kapolei	HI	Hawaii	21.324	-158.089	17	suburban
160010010	Meridian	ID	Northwest	43.601	-116.348	826	urban
170310057	Chicago	IL	Chicago	41.915	-87.723	185	suburban
170310076	Chicago	IL	Chicago	41.751	-87.714	188	suburban
170314201	Northbrook	IL	Chicago	42.14	-87.799	194	suburban
170434002	Naperville	IL	Chicago	41.771	-88.153	213	urban
171190024	Granite City	IL	Central U.S.	38.701	-90.145	128	urban
180190006	Jefferson	IN	Ohio River Valley	38.278	-85.74	137	urban
180372001	Jasper	IN	Ohio River Valley	38.391	-86.929	139	urban
180650003	Middleton	IN	Ohio River Valley	40.012	-85.524	309	rural
180890022	Gary	IN	Michigan/Great Lakes	41.607	-87.305	179	urban
180970078	Indianapolis	IN	Ohio River Valley	39.811	-86.115	240	suburban
181630021	Evansville	IN	Ohio River Valley	38.013	-87.577	116	urban

Site	City	State	Region	Latitude	Longitude	Elevation (m)	Setting
191630015	Davenport	IA	Central U.S.	41.53	-90.588	212	urban
201730010	Wichita	KS	Central U.S.	37.701	-97.314	405	urban
202090021	Kansas City	KS	Central U.S.	39.118	-94.636	269	urban
211110067	Louisville	KY	Ohio River Valley	38.229	-85.654	127	suburban
220330009	Baton Rouge	LA	East Texas/Gulf	30.461	-91.177	16	urban
240053001	Essex	MD	Washington D.C./ Philadelphia Corridor	39.311	-76.474	10	suburban
240330030	Beltsville	MD	Washington D.C./ Philadelphia Corridor	39.055	-76.878	47	suburban
250130008	Westover AFB	MA	Northeast	42.195	-72.556	60	suburban
250250042	Boston	MA	Northeast	42.329	-71.083	5	urban
260810020	Grand Rapids	MI	Michigan/Great Lakes	42.984	-85.671	190	urban
260910007	Tecumseh	MI	Michigan/Great Lakes	41.996	-83.947	0	suburban
261630001	Allen Park	MI	Michigan/Great Lakes	42.229	-83.208	182	suburban
261630015	Detroit	MI	Michigan/Great Lakes	42.303	-83.107	180	urban
261630033	Detroit	MI	Michigan/Great Lakes	42.307	-83.149	179	suburban
270031002	Blaine	MN	Central U.S.	45.138	-93.208	280	suburban
270530963	Minneapolis	MN	Central U.S.	44.955	-93.258	265	urban
280490020	Jackson	MS	Southeast	32.329	-90.183	106	urban
290990019	Arnold	MO	Central U.S.	38.449	-90.396	195	suburban
295100085	St. Louis	MO	Central U.S.	38.656	-90.198	144	urban
300490004	Helena	MT	Northwest	46.851	-111.987	1194	rural
300930005	Butte	MT	Northwest	46.003	-112.501	1682	urban
310550019	Omaha	NE	Central U.S.	41.247	-95.976	347	suburban
320030540	Las Vegas	NV	Las Vegas	36.412	-115.079	610	urban
320310016	Reno	NV	Northwest Nevada	39.525	-119.808	1403	urban
340070002	Camden	NJ	Northeast	39.934	-75.125	4	urban
340130003	Newark	NJ	Northeast	40.721	-74.193	27	urban
340230011	Rutgers	NJ	Northeast	40.462	-74.429	19	rural
340273001	Chester	NJ	Northeast	40.788	-74.676	256	rural
340390004	Elizabeth	NJ	Northeast	40.641	-74.208	3	suburban
350010023	Albuquerque	NM	Albuquerque	35.134	-106.586	1578	urban
360010005	Albany	NY	Northeast	42.642	-73.755	7	urban
360050110	Bronx	NY	New York City	40.816	-73.902	14	urban
360290005	Buffalo	NY	Northeast	42.877	-78.81	186	urban
360310003	Wilmington	NY	Northeast	44.393	-73.859	584	rural
360551007	Rochester	NY	Northeast	43.146	-77.548	146	urban
360610134	New York City	NY	New York City	40.714	-73.996	5	urban
360810124	Queens	NY	New York City	40.736	-73.823	13	suburban
361010003	Addison	NY	Northeast	42.091	-77.21	490	rural
370670022	Winston-Salem	NC	Southeast	36.111	-80.227	279	urban
371190041	Charlotte	NC	Southeast	35.24	-80.786	223	urban
371830014	Raleigh	NC	Southeast	35.856	-78.574	92	suburban
380150003	Bismarck	ND	North Dakota	46.825	-100.768	548	suburban
390350038	Cleveland	OH	Ohio River Valley	41.477	-81.682	186	urban
390350060	Cleveland	OH	Michigan/Great Lakes	41.494	-81.679	197	urban

Site	City	State	Region	Latitude	Longitude	Elevation (m)	Setting
390350065	Newburgh Heights	OH	Ohio River Valley	41.447	-81.662	210	urban
390350076	Cuyahoga Heights	OH	Ohio River Valley	41.424	-81.648	182	urban
390610040	Cincinnati	OH	Ohio River Valley	39.129	-84.504	213	urban
390810017	Stuebenville	OH	Ohio River Valley	40.366	-80.616	222	urban
390933002	Sheffield	OH	Michigan/Great Lakes	41.463	-82.114	182	suburban
391130038	Sinclair	OH	Ohio River Valley	39.756	-84.199	220	urban
391351001	New Paris	OH	Ohio River Valley	39.836	-84.721	357	rural
391510017	Canton	OH	Ohio River Valley	40.787	-81.394	334	urban
391530023	Akron	OH	Ohio River Valley	41.088	-81.542	313	urban
401091037	Edmond	OK	Midsouth	35.614	-97.475	344	suburban
401431127	Tulsa	OK	Midsouth	36.205	-95.977	193	urban
410510080	Portland	OR	Oregon	45.497	-122.602	86	suburban
420010001	Arendtsville	PA	Northeast	39.92	-77.31	241	rural
420030008	Pittsburgh	PA	Ohio River Valley	40.466	-79.961	312	suburban
420030064	Liberty	PA	Ohio River Valley	40.324	-79.868	279	suburban
420210011	Johnstown	PA	Ohio River Valley	40.31	-78.915	361	urban
420290100	Toughkenamon	PA	Washington D.C./ Philadelphia Corridor	39.834	-75.769	91	rural
420450002	Chester	PA	Washington D.C. /Philadelphia Corridor	39.836	-75.373	3	urban
420450109	Marcus Hook	PA	Washington D.C. /Philadelphia Corridor	39.819	-75.414	0	urban
420710007	Lancaster	PA	Northeast	40.047	-76.283	99	suburban
420710012	Intercourse	PA	Northeast	40.044	-76.112	116	suburban
421010048	Philadelphia	PA	Washington D.C./ Philadelphia Corridor	39.923	-75.098	25	urban
421010055	Philadelphia	PA	Washington D.C./ Philadelphia Corridor	39.923	-75.187	3	urban
421255001	Burgettstown	PA	Ohio River Valley	40.445	-80.421	344	rural
421290008	Greensburg	PA	Ohio River Valley	40.305	-79.506	378	suburban
440071010	Rumford	RI	Northeast	41.841	-71.361	15	suburban
460990008	Sioux Falls	SD	Central U.S.	43.548	-96.701	451	urban
470931020	Knoxville	TN	Southeast	36.019	-83.874	309	suburban
471570075	Memphis	TN	Southeast	35.152	-89.85	87	suburban
481130069	Dallas	TX	Dallas	32.82	-96.86	132	urban
481410044	El Paso	TX	West Texas/El Paso	31.766	-106.455	1122	urban
482011039	Deer Park	TX	East Texas/Gulf	29.67	-95.129	9	suburban
482030002	Karnack	TX	Midsouth	32.669	-94.168	72	rural
490110004	Bountiful	UT	Utah	40.903	-111.885	1307	suburban
490353006	Salt Lake City	UT	Utah	40.736	-111.872	1309	suburban
490494001	Lindon	UT	Utah	40.341	-111.714	1456	suburban
500070012	Burlington	VT	Northeast	44.48	-73.214	42	urban
510870014	Richmond	VA	Southeast	37.558	-77.4	34	suburban
530330030	Seattle	WA	Puget Sound	47.597	-122.32	15	urban
530330080	Seattle	WA	Puget Sound	47.57	-122.309	58	urban
530530029	Tacoma	WA	Puget Sound	47.186	-122.452	97	suburban
530770009	Yakima	WA	Northwest	46.598	-120.499	326	urban
540390020	Charleston	WV	Ohio River Valley	38.346	-81.621	223	urban
540511002	Moundsville	WV	Ohio River Valley	39.916	-80.734	245	suburban

Site	City	State	Region	Latitude	Longitude	Elevation (m)	Setting
550090005	Green Bay	WI	Central U.S.	44.507	-87.993	184	urban
550270001	Horicon	WI	Central U.S.	43.466	-88.621	287	rural
550790026	Milwaukee	WI	Central U.S.	43.061	-87.913	216	urban
551198001	Perkinstown	WI	Central U.S.	45.204	-90.6	449	rural
560210100	Cheyenne	WY	Front Range CO	41.182	-104.778	15	suburban

The IMPROVE and CSN networks operate collocated samplers in several urban/suburban sites. Collocated sites with data that met the completeness criteria outlined in Chapter 2 were compared to identify relative biases between IMPROVE and CSN speciated aerosol concentrations. Monthly mean data from Birmingham, Alabama; Fresno, California; Phoenix, Arizona; and Puget Sound, Washington, for 2016–2019 were compared for ammonium sulfate (AS), AN, OC, EC, fine dust, sea salt (SS), $PM_{2.5}$ gravimetric fine mass (FM), and reconstructed fine mass (RCFM). Descriptions of species mass concentrations calculations are listed in Table 2.1 in Chapter 2.

Scatter plots of comparisons between IMPROVE and CSN species mass concentrations are presented in Figure 1.16. A summary of results is provided in Table 1.9. Errors were less than 20% for most species, with the exception of fine dust (21%) and sea salt (85%). IMPROVE SS concentrations were computed using chloride ion concentrations ($1.8\times Cl^-$), whereas CSN SS concentrations were computed using chlorine concentrations ($1.8\times Cl$) from XRF analysis. (CSN began reporting chloride concentrations in February 2017). Errors for EC were 19%, in part due to TOR hardware changes for CSN. Biases were typically within ±15%, except for a -20% bias in fine dust (IMPROVE higher), -81% bias in SS (IMPROVE higher), and 21% bias in EC (CSN higher). Higher biases and errors associated with coarse-mode species may be due in part to differences in the sharpness of the cut points between IMPROVE and CSN samplers, with sharper CSN cut points resulting in lower concentrations, because less of the tail of the coarse-mode species is collected by the $PM_{2.5}$ filter. Additional comparisons between IMPROVE and CSN data are described in Gorham et al. (2021).

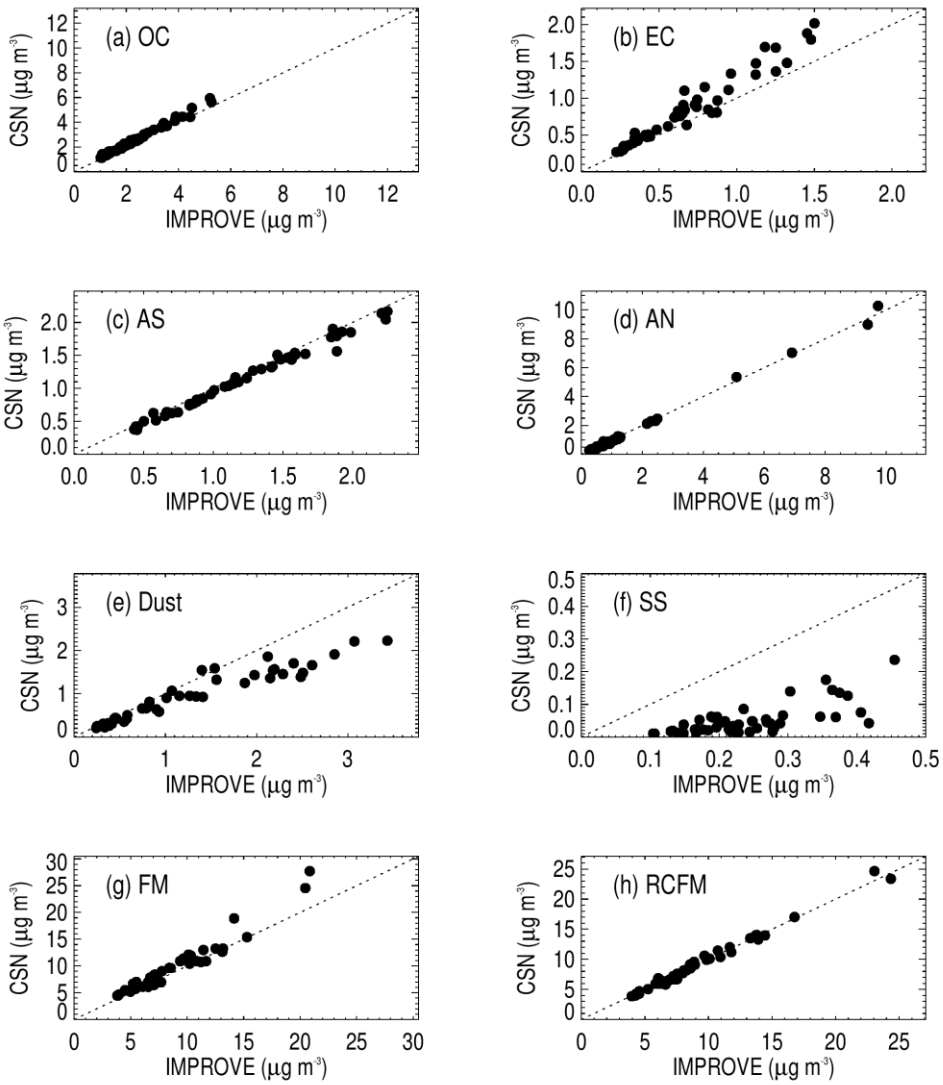

Figure 1.16. Comparisons of monthly mean 2016–2019 $PM_{2.5}$ aerosol mass concentration data (µg m^{-3}) for four collocated IMPROVE and CSN sites (see text) for (a) organic carbon (OC), (b) elemental carbon (EC), (c) ammonium sulfate (AS), (d) ammonium nitrate (AN), (e) fine dust, (f) sea salt (SS), (g) $PM_{2.5}$ gravimetric fine mass (FM), and (h) reconstructed fine mass (RCFM).

Table 1.9. Comparisons between monthly mean data at collocated IMPROVE and CSN sites from 2016 through 2019. Species include organic carbon (OC), elemental carbon (EC), ammonium sulfate (AS), ammonium nitrate (AN), fine dust (FD), sea salt (SS), $PM_{2.5}$ gravimetric fine mass (FM), and $PM_{2.5}$ reconstructed fine mass (RCFM). Positive biases correspond to higher CSN concentrations.

Statistic	OC	EC	AS[3]	AN[4]	Dust	Sea salt[5]	FM	RCFM
Average IMPROVE (µg m^{-3})	2.36	0.69	1.21	1.44	1.21	0.24	8.58	9.04
Average CSN (µg m^{-3})	2.59	0.84	1.15	1.40	0.90	0.05	9.42	9.01
Bias[1] (%)	11	21	-6	-6	-20	-81	9	-1
Error[2] (%)	11	19	6	8	21	85	10	4
r	0.99	0.97	0.99	1.00	0.96	0.71	0.97	0.99
IMP/CSN	0.91	0.82	1.06	1.03	1.34	4.75	0.91	1.00

[1] $\text{Error} = \text{median}\left(\left|\frac{\overline{X}_i - \overline{Y}_i}{\overline{Y}_i}\right|\right)$

[2] $\text{Bias} = \frac{1}{N}\sum_{i}^{N}\frac{\overline{X}_i - \overline{Y}_i}{\overline{Y}_i}$; $\overline{X}_i$ and $\overline{Y}_i$ are the daily data for CSN and IMPROVE concentrations, respectively. N gives the number of data points.

[3] AS = 1.375×[sulfate ion]

[4] AN = 1.29×[nitrate ion]

[5] Sea salt = 1.8×[chloride ion] for IMPROVE and 1.8×[chlorine] for CSN.

REFERENCES

Chen, L.-W., Chow, J., Wang, X., Robles, J., Sumlin, B., Lowenthal, D., Zimmermann, R., and Watson, J. (2015), Multi-wavelength optical measurement to enhance thermal/optical analysis for carbonaceous aerosol, *Atmospheric Measurement Techniques*, *8*(1), 451-461, doi:doi:10.5194/amt-8-451-2015.

Chen, L.-W. A., Chow, J. C., Wang, X., Cao, J., Mao, J., and Watson, J. G. (2021), Brownness of organic aerosol over the United States: Evidence for seasonal biomass burning and photobleaching effects, *Environmental Science & Technology*, *55*(13), 8561-8572, doi:10.1021/acs.est.0c08706.

Cheng, X. (2015), Changes in redelivery of 1/2005 through 5/2014 data, *IMPROVE Data Advisory*(da0031), http://vista.cira.colostate.edu/improve/Data/QA_QC/Advisory/da0031/da0031_2010to2014Redelivery.pdf.

Chow, J. C., Watson, J. G., Pritchett, L. C., Pierson, W. R., Frazier, C. A., and Purcell, R. G. (1993), The DRI thermal/optical reflectance carbon analysis system: description, evaluation and applications in US air quality studies, *Atmospheric Environment. Part A. General Topics*, *27*(8), 1185-1201, https://doi.org/10.1016/0960-1686(93)90245-T.

Chow, J. C., Watson, J. G., Crow, D., Lowenthal, D. H., and Merrifield, T. (2001), Comparison of IMPROVE and NIOSH carbon measurements, *Aerosol Science & Technology*, *34*(1), 23-34, doi:10.1080/02786820600623711.

Chow, J. C., Watson, J. G., Chen, L.-W. A., Arnott, W. P., Moosmüller, H., and Fung, K. (2004), Equivalence of elemental carbon by thermal/optical reflectance and transmittance with different temperature protocols, *Environmental Science & Technology*, *38*(16), 4414-4422, doi:10.1021/es034936u.

Chow, J. C., Watson, J. G., Chen, L.-W. A., Chang, M., and Paredes-Miranda, G. (2005), Comparison of the DRI/OGC and Model 2001 thermal/optical carbon analyzers, *Prepared for IMPROVE Steering Committee, Fort Collins, CO, by Desert Research Institute, Reno, NV*, http://vista.cira.colostate.edu/improve/Publications/GrayLit/013_CarbonAnalyzer/IMPROVECarbonAnalyzerAssessment.pdf.

Chow, J. C., Watson, J. G., Chen, L.-W. A., Chang, M. O., Robinson, N. F., Trimble, D., and Kohl, S. (2007), The IMPROVE_A temperature protocol for thermal/optical carbon analysis: maintaining consistency with a long-term database, *Journal of the Air & Waste Management Association*, *57*(9), 1014-1023, https://doi.org/10.3155/1047-3289.57.9.1014.

Chow, J., Watson, J., Chen, L.-W., Rice, J., and Frank, N. (2010), Quantification of PM 2.5 organic carbon sampling artifacts in US networks, *Atmospheric Chemistry and Physics*, *10*(12), 5223-5239, doi:https://doi.org/10.5194/acp-10-5223-2010.

Chow, J. C., Wang, X., Sumlin, B. J., Gronstal, S. B., Chen, L.-W. A., Trimble, D. L., Kohl, S. D., Mayorga, S. R., Riggio, G., and Hurbain, P. R. (2015a), Optical calibration and equivalence of a multiwavelength thermal/optical carbon analyzer, *Aerosol and Air Quality Research*, *15*(4), 1145-1159, doi:10.4209/aaqr.2015.02.0106.

Chow, J. C., Lowenthal, D. H., Chen, L.-W. A., Wang, X., and Watson, J. G. (2015b), Mass reconstruction methods for PM2. 5: a review, *Air Quality, Atmosphere & Health*, *8*(3), 243-263, doi:10.1007/s11869-015-0338-3.

Chow, J. C., Watson, J. G., Green, M. C., Wang, X., Chen, L.-W. A., Trimble, D. L., Cropper, P. M., Kohl, S. D., and Gronstal, S. B. (2018), Separation of brown carbon from black carbon for IMPROVE and Chemical Speciation Network PM2. 5 samples, *Journal of the Air & Waste Management Association*, *68*(5), 494-510, doi:https://doi.org/10.1080/10962247.2018.1426653.

Chow, J. C., Chen, L.-W. A., Wang, X., Green, M. C., and Watson, J. G. (2021), Improved estimation of PM2. 5 brown carbon contributions to filter light attenuation, *Particuology*, *56*, 1-9, doi:10.1016/j.partic.2021.01.001.

Debell, L. J., Gebhart, K., Hand, J. L., Malm, W. C., Pitchford, M. L., Schichtel, B. S., and White, W. H. (2006), IMPROVE (Interagency Monitoring of Protected Visual Environments): Spatial and seasonal patterns and temporal variability of haze and its constituents in the United States: Report IV, Colorado State University, Fort Collins CO, ISSN 0737-5352-74.

Debus, B., Takahama, S., Weakley, A. T., Seibert, K., and Dillner, A. M. (2019), Long-term strategy for assessing carbonaceous particulate matter concentrations from multiple Fourier transform infrared (FT-IR) instruments: influence of spectral dissimilarities on multivariate calibration performance, *Applied Spectroscopy*, *73*(3), 271-283.

Debus, B., Weakley, A. T., Takahama, S., George, K. M., Schichtel, B. A., Copeland, S., Wexler, A. S., and Dillner, A. M. (submitted), Quantification of major particulate matter species from a single filter type using infrared spectroscopy – Application to a large-scale monitoring network, *Atmospheric Measurement Techniques Discussion*.

Dewangan, S., Pervez, S., Chakrabarty, R., Watson, J. G., Chow, J. C., Pervez, Y., Tiwari, S., and Rai, J. (2016), Study of carbonaceous fractions associated with indoor PM2. 5/PM10 during Asian cultural and ritual burning practices, *Building and Environment*, *106*, 229-236, https://doi.org/10.1016/j.buildenv.2016.06.006.

Dillner, A. M., Phuah, C. H., and Turner, J. R. (2009), Effects of post-sampling conditions on ambient carbon aerosol filter measurements, *Atmospheric Environment*, *43*(37), 5937-5943, https://doi.org/10.1016/j.atmosenv.2009.08.009.

Dillner, A. (2015), Change to artifact correction method for OC carbon fractions, *IMPROVE Data Advisory* (da0032), http://vista.cira.colostate.edu/improve/Data/QA_QC/Advisory/da0032/da0032_OC_artifact.pdf.

Dillner, A. M., and Takahama, S. (2015a), Predicting ambient aerosol thermal-optical reflectance (TOR) measurements from infrared spectra: organic carbon, *Atmos. Meas. Tech.*, *8*(3), 1097-1109, doi:10.5194/amt-8-1097-2015.

Dillner, A. M., and Takahama, S. (2015b), Predicting ambient aerosol thermal–optical reflectance measurements from infrared spectra: elemental carbon, *Atmos. Meas. Tech.*, *8*(10), 4013-4023, doi:10.5194/amt-8-4013-2015.

EPA, U. S. (1999a), U.S. Environmental Protection Agency, Regional Haze Rule regulations, *Final Rule*, *40 CFR 51*(Federal Register, 64), 35714-35774, https://www.govinfo.gov/content/pkg/FR-1999-07-01/pdf/99-13941.pdf.

EPA, U. S. (1999b), U.S. Environmental Protection Agency, Visibility Monitoring Guidance, *EPA-454/R-99-003*.

EPA, U. S. (2004), U.S. Environmental Protection Agency, PM2.5 Speciation Network Newsletter, *1*(1), https://www3.epa.gov/ttnamti1/files/ambient/pm25/spec/spnews1.pdf.

EPA, U. S. (2009), U.S. Environmental Protection Agency, PM2.5 Speciation Network Newsletter, *1*(6), https://www3.epa.gov/ttnamti1/files/ambient/pm25/spec/spnews6.pdf.

EPA, U. S. (2018), U.S. Environmental Protection Agency, Technical guidance on tracking visibility progress for the second implementation period of the Regional Haze program, *EPA-454/R-18-010*.

Gorham, K. A., Raffuse, S. M., Hyslop, N. P., and White, W. H. (2021), Comparison of recent speciated PM2. 5 data from collocated CSN and IMPROVE measurements, *Atmospheric Environment*, *244*, 117977, https://doi.org/10.1016/j.atmosenv.2020.117977.

Hand, J. L., Copeland, S., Day, D., Dillner, A., Indresand, H., Malm, W., McDade, C., Moore, C., Pitchford, M., and Schichtel, B. (2011), IMPROVE (Interagency Monitoring of Protected Visual Environments): Spatial and seasonal patterns and temporal variability of haze and its constituents in the United States, Report V, Colorado State University, Fort Collins, CO.

Hand, J. L., Schichtel, B. A., Pitchford, M., Malm, W. C., and Frank, N. H. (2012), Seasonal composition of remote and urban fine particulate matter in the United States, *Journal of Geophysical Research: Atmospheres*, *117*(D5), D05209, doi:10.1029/2011jd017122.

Hand, J. L., Prenni, A. J., Schichtel, B. A., Malm, W. C., and Chow, J. C. (2019), Trends in remote PM2.5 residual mass across the United States: Implications for aerosol mass reconstruction in the IMPROVE network, *Atmospheric Environment*, *203*, 141-152, doi:doi:10.1016/j.atmosenv.2019.01.049.

Joseph, D., Metsa, J., Malm, W. C., and Pitchford, M. (1987), Plans for IMPROVE: A federal program to monitor visibility in class I areas, in *Visibility Protection: Research and Policy Aspects,* Bhardwaja, P. S. (ed), APCA, Pittsburgh, PA.

June, N. A., Wang, X., Chen, L. W. A., Chow, J. C., Watson, J. G., Wang, X., Henderson, B. H., Zheng, Y., and Mao, J. (2020), Spatial and temporal variability of brown carbon in the United States: Implications for direct radiative effects, *Geophysical Research Letters*, *47*(23), e2020GL090332, doi:10.1029/2020GL090332.

Kim, E., and Hopke, P. K. (2004), Comparison between conditional probability function and nonparametric regression for fine particle source directions, *Atmospheric Environment*, *38*(28), 4667-4673, https://doi.org/10.1016/j.atmosenv.2004.05.035.

Kim, E., Hopke, P. K., Larson, T. V., Maykut, N. N., and Lewtas, J. (2004), Factor analysis of Seattle fine particles, *Aerosol Science and Technology*, *38*(7), 724-738, https://doi.org/10.1080/02786820490490119.

Li, S., Zhu, M., Yang, W., Tang, M., Huang, X., Yu, Y., Fang, H., Yu, X., Yu, Q., and Fu, X. (2018), Filter-based measurement of light absorption by brown carbon in PM2. 5 in a megacity in South China, *Science of The Total Environment*, *633*, 1360-1369, doi:10.1016/j.scitotenv.2018.03.235.

Malm, W. C., Sisler, J. F., Huffman, D., Eldred, R. A., and Cahill, T. A. (1994), Spatial and seasonal trends in particle concentration and optical extinction in the United States, *Journal of Geophysical Research: Atmospheres*, *99*(D1), 1347-1370, https://doi.org/10.1029/93JD02916.

Malm, W., Sisler, J. F., Pitchford, M., Scruggs, M., Ames, R. B., Copeland, S., Gebhart, K., and Day, D. (2000), IMPROVE (Interagency Monitoring of Protected Visual Environments): Spatial and seasonal patterns and temporal variability of haze and its constituents in the United States: Report III, Colorado State University, Fort Collins, CO, ISSN 0737-5352-47.

Malm, W. C., Schichtel, B. A., and Pitchford, M. L. (2011), Uncertainties in PM2. 5 gravimetric and speciation measurements and what we can learn from them, *Journal of the Air & Waste Management Association*, *61*(11), 1131-1149, doi:10.1080/10473289.2011.603998.

Molenar, J. V., Dietrich, D. L., and Tree, R. M. (1989), Application of a long-range transmissometer to measure the ambient atmospheric extinction coefficient in remote pristine environments, in *Visibility and Fine Particles*, Mathai, C. V. (ed), 374-383, A&WMA, Pittsburgh, PA.

Molenar, J., and Malm, W. (1992), Ambient optical monitoring techniques, in *Proceedings of Conference on Visibility and Fine Particles*, Vienna.

Petzold, A., Ogren, J. A., Fiebig, M., Laj, P., Li, S. M., Baltensperger, U., Holzer-Popp, T., Kinne, S., Pappalardo, G., Sugimoto, N., Wehrli, C., Wiedensohler, A., and Zhang, X. Y. (2013), Recommendations for reporting "black carbon" measurements, *Atmos. Chem. Phys.*, *13*(16), 8365-8379, doi:10.5194/acp-13-8365-2013.

Pitchford, M., Malm, W. C., Schichtel, B. A., Kumar, N., Lowenthal, D., and Hand, J. L. (2007), Revised algorithm for estimating light extinction from IMPROVE particle speciation data, *Journal of the Air & Waste Management Association*, *57*(11), 1326-1336, doi:10.3155/1047-3289.57.11.1326.

Reggente, M., Dillner, A. M., and Takahama, S. (2016), Predicting ambient aerosol thermal–optical reflectance (TOR) measurements from infrared spectra: Extending the predictions to different years and different sites, *Atmos. Meas. Tech.*, *9*(2), 441-454, doi:10.5194/amt-9-441-2016.

Schichtel, B. A. (2019), Updated data for carbon, *IMPROVE Data Advisory* (da0040), http://vista.cira.colostate.edu/improve/Data/QA_QC/Advisory/da0040/da0040_TOR_integration.pdf.

Schichtel, B. A., Malm, W. C., Beaver, M., Copeland, S., Hand, J. L., Prenni, A. J., Rice, J., and Vimont, J. (2021), The Future of Carbonaceous Aerosol Measurement in the IMPROVE Monitoring Program, http://vista.cira.colostate.edu/improve/wp-content/uploads/2021/10/041_CarbonReport_Final.pdf.

Shen, Z., Lei, Y., Zhang, L., Zhang, Q., Zeng, Y., Tao, J., Zhu, C., Cao, J., Xu, H., and Liu, S. (2017), Methanol extracted brown carbon in PM2. 5 over Xi'an, China: Seasonal variation of optical properties and sources identification, *Aerosol Science and Engineering*, *1*(2), 57-65, doi:10.1007/s41810-017-0007-z.

Shibata, K., Enya, K., Ishikawa, N., and Sakamoto, K. (2019), EC/OC and PAHs emissions from a modern diesel engine with DPF regeneration fueled by 10% RME biodiesel, *Aerosol and Air Quality Research*, *19*(8), 1765-1774, doi:10.4209/aaqr.2018.12.0476.

Solomon, P. A., Crumpler, D., Flanagan, J. B., Jayanty, R. K. M., Rickman, E. E., and McDade, C. E. (2014), U.S. national PM2.5 chemical speciation monitoring networks—CSN and IMPROVE: Description of networks, *Journal of the Air & Waste Management Association*, *64*(12), 1410-1438, doi:10.1080/10962247.2014.956904.

Takahama, S., Dillner, A. M., Weakley, A. T., Reggente, M., Bürki, C., Lbadaoui-Darvas, M., Debus, B., Kuzmiakova, A., and Wexler, A. S. (2019), Atmospheric particulate matter characterization by Fourier transform infrared spectroscopy: a review of statistical calibration strategies for carbonaceous aerosol quantification in US measurement networks, *Atmospheric Measurement Techniques*, *12*(1), 525-567, https://doi.org/10.5194/amt-12-525-2019.

Trzepla, K. (2018), Calibration bias in reported vanadium concentrations, *IMPROVE Data Advisory* (da0038), http://vista.cira.colostate.edu/improve/Data/QA_QC/Advisory/da0038/da0038_V_advisory.pdf.

Trzepla, K. (2019), Change in the analytical protocol for XRF analysis, *IMPROVE Data Advisory* (da0043), http://vista.cira.colostate.edu/improve/Data/QA_QC/Advisory/da0043/da0043_XRFprotocolChange2019.pdf.

Trzepla, K., and Giacomo, J. (2019), Changes/upgrades in HIPS system resulting in calibration changes, *IMPROVE Data Advisory* (da0041), http://vista.cira.colostate.edu/improve/Data/QA_QC/Advisory/da0041/da0041_HIPSmodifications.pdf.

Turpin, B. J., Saxena, P., and Andrews, E. (2000), Measuring and simulating particulate organics in the atmosphere: problems and prospects, *Atmospheric Environment*, *34*(18), 2983-3013, https://doi.org/10.1016/S1352-2310(99)00501-4.

Wagner, J. G., Kamal, A. S., Morishita, M., Dvonch, J. T., Harkema, J. R., and Rohr, A. C. (2014), PM2.5-induced cardiovascular dysregulation in rats is associated with elemental carbon and temperature-resolved carbon subfractions, *Particle and Fibre Toxicology*, *11*(1), 25, doi:10.1186/1743-8977-11-25.

Wallis, C. (2019a), Method change for calibrating flow rate transfer standards, *IMPROVE Data Advisory* (da0042), http://vista.cira.colostate.edu/improve/Data/QA_QC/Advisory/da0042/da0042_FlowrateTransferStandardCalibrationProtocol.pdf.

Wallis, C. (2019b), Universal calibration constants for flow rate calculation, *IMPROVE Data Advisory* (da0044), http://vista.cira.colostate.edu/improve/Data/QA_QC/Advisory/da0044/da0044_UniversalFlowRateCalibrationConstants.pdf.

Watson, J., Lioy, P., and Mueller, P. (2001), The measurement process: Precision, accuracy, and validity, *Air sampling instruments for evaluation of atmospheric contaminants*, *8*.

Watson, J. G., Chow, J. C., Chen, L.-W. A., and Frank, N. H. (2009), Methods to assess carbonaceous aerosol sampling artifacts for IMPROVE and other long-term networks, *Journal of the Air & Waste Management Association*, *59*(8), 898-911, https://doi.org/10.3155/1047-3289.59.8.898.

White, W. H. (2007), Shift in EC/OC split with 1 January 2005 TOR hardware upgrade, *IMPROVE Data Advisory* (da0016), http://vista.cira.colostate.edu/improve/Data/QA_QC/Advisory/da0016/da0016_TOR2005.pdf.

White, W. H. (2009), Under-correction of chloride concentrations for filter blank levels, *IMPROVE Data Advisory* (da0024), http://vista.cira.colostate.edu/improve/Data/QA_QC/Advisory/da0024/da0024_HDA_Chloride.pdf.

White, W. H. (2015a), Changed reporting of light absorption, *IMPROVE Data Advisory* (da0033), http://vista.cira.colostate.edu/improve/Data/QA_QC/Advisory/da0033/da0033_Fabs.pdf.

White, W. H. (2015b), Bias between masked and unmasked light absorption measurements, *IMPROVE Data Advisory* (da0034), http://vista.cira.colostate.edu/improve/Data/QA_QC/Advisory/da0034/da0034_update-mask-Fabs.pdf.

White, W. H. (2016), Increased variation of humidity in the weighing laboratory, *IMPROVE Data Advisory* (da0035), http://vista.cira.colostate.edu/improve/Data/QA_QC/Advisory/da0035/da0035_IncreasedRH.pdf.

White, W. H., Trzepla, K., Hyslop, N. P., and Schichtel, B. A. (2016), A critical review of filter transmittance measurements for aerosol light absorption, and de novo calibration for a decade of monitoring on PTFE membranes, *Aerosol Science and Technology*, *50*(9), 984-1002, http://dx.doi.org/10.1080/02786826.2016.1211615.

White, W. H. (2017a), Negative chloride concentrations at salt-poor sites, *IMPROVE Data Advisory* (da0036), http://vista.cira.colostate.edu/improve/Data/QA_QC/Advisory/da0036/da0036_chloride_loss.pdf

White, W. H. (2017b), Over-reporting of sodium in salt-rich samples, *IMPROVE Data Advisory* (da0037), http://vista.cira.colostate.edu/improve/Data/QA_QC/Advisory/da0037/da0037_Na_matrix.pdf.

Yu, X.-Y., Lee, T., Ayres, B., Kreidenweis, S. M., Collett Jr, J. L., and Malm, W. (2005), Particulate nitrate measurement using nylon filters, *Journal of the Air & Waste Management Association*, *55*(8), 1100-1110, https://doi.org/10.1080/10473289.2005.10464721.

Zhang, X. (2019), Correction of chloride concentrations for filter blank levels, *IMPROVE Data Advisory* (da0039), http://vista.cira.colostate.edu/improve/Data/QA_QC/Advisory/da0039/da0039_ChlorideOverCorrection.pdf.